



<https://theses.gla.ac.uk/>

Theses Digitisation:

<https://www.gla.ac.uk/myglasgow/research/enlighten/theses/digitisation/>

This is a digitised version of the original print thesis.

Copyright and moral rights for this work are retained by the author

A copy can be downloaded for personal non-commercial research or study,
without prior permission or charge

This work cannot be reproduced or quoted extensively from without first
obtaining permission in writing from the author

The content must not be changed in any way or sold commercially in any
format or medium without the formal permission of the author

When referring to this work, full bibliographic details including the author,
title, awarding institution and date of the thesis must be given

Enlighten: Theses

<https://theses.gla.ac.uk/>
research-enlighten@glasgow.ac.uk

THE INTERSTELLAR POLARIZATION LAW

Thesis
submitted to the
University of Glasgow
for the degree of
M.Sc.

by

Alia H. Al-Roubaie

Department of Astronomy
University of Glasgow

October
1981

ProQuest Number: 10753797

All rights reserved

INFORMATION TO ALL USERS

The quality of this reproduction is dependent upon the quality of the copy submitted.

In the unlikely event that the author did not send a complete manuscript and there are missing pages, these will be noted. Also, if material had to be removed, a note will indicate the deletion.



ProQuest 10753797

Published by ProQuest LLC (2018). Copyright of the Dissertation is held by the Author.

All rights reserved.

This work is protected against unauthorized copying under Title 17, United States Code
Microform Edition © ProQuest LLC.

ProQuest LLC.
789 East Eisenhower Parkway
P.O. Box 1346
Ann Arbor, MI 48106 – 1346

TO MY PARENTS

*for their
constant encouragement*

C O N T E N T S

	Page No.
ACKNOWLEDGEMENTS	1
FOREWORD	2
1. CHAPTER 1	3
HISTORICAL REVIEW OF INTERSTELLAR POLARIZATION	
1.1 Introduction	4
1.2 Interstellar Polarization	5
1.3 Wavelength Dependence of Interstellar Polarization	6
1.4 Intrinsic Polarization	22
2. CHAPTER 2	27
REASSESSMENT OF THE INTERSTELLAR POLARIZATION LAW	
2.1 Introduction	28
2.2 Analysis of the Data	29
3. CHAPTER 3	41
A NUMERICAL INVESTIGATION OF NOISY POLARIMETRIC DATA	
3.1 The Computer Programme Scheme	42
3.2 Analysis of Simulated Noisy Data	43
4. CHAPTER 4	49
THE ROTATION OF POLARIZATION POSITION ANGLE WITH WAVELENGTH	
4.1 Introduction	50
4.2 The Two-Cloud Model	51
4.3 The Stars Displaying $\theta(\lambda)$	56
5. CHAPTER 5	62
A NUMERICAL INVESTIGATION OF THE TWO-CLOUD MODEL	
5.1 Introduction	63
5.2 The Two-Cloud Model	63

CONTENTS, continued

	Page No.
GENERAL SUMMARY	82
APPENDIX 1 The Values of K and λ_{\max} for SMF Data	85
APPENDIX 2 The Values of K and λ_{\max} for CGS Data	87
REFERENCES TO FIGURES	89
REFERENCES	90

A C K N O W L E D G M E N T S

I wish to acknowledge Professor P. A. Sweet for the facilities in his department.

I gratefully acknowledge my supervisor Dr D. Clarke for initiating and sustaining my interest in the fields of the research discussed in this thesis. His enthusiastic advice and comments on the manuscript with informative and fruitful discussions were indispensable and are deeply appreciated.

Many thanks are due to Mrs. M. I. Morris for her invaluable and careful typing of the thesis and production of the diagrams; her helpful work, which has put a final polish on the presentation, is very much appreciated.

This work has been granted by the Iraqi Ministry of Higher Education and Scientific Research.

FOREWORD

The work discussed in this thesis aimed to investigate the interstellar polarization law $[p(\lambda)/p_{\max} = \exp(-K \ln^2(\lambda_{\max}/\lambda))]$ and the behaviour of its characteristic parameters, K and λ_{\max} , in both simple and complex cloud situations, i.e. for stars exhibiting rotation of polarization position angle, $\theta(\lambda)$.

As the law is difficult to deal with analytically, the work is here mainly based on numerical investigations.

Chapter 1 contains a general review of starlight polarization including intrinsic linear and interstellar linear and circular forms but the main theme concentrates on interstellar linear polarization.

In Chapter 2 existing data have been refitted to the interstellar polarization law using the method of the least squares.

In Chapter 3 a numerical investigation has been made of the effect that noisy data have on deduced parameters such as K and λ_{\max} .

Chapter 4 contains a brief review of data for stars showing $\theta(\lambda)$ with discussions of the different cloud models, especially Martin's Two-Cloud model.

In Chapter 5 numerical investigations are presented of the Two-Cloud model with analysis of the results for different configurations of the two clouds. A general summary is placed at the end of the thesis.

CHAPTER 1

HISTORICAL REVIEW OF INTERSTELLAR POLARIZATION

1.1 Introduction

1.2 Interstellar Polarization

1.3 Wavelength Dependence of Interstellar Polarization

1.4 Intrinsic Polarization

1.1 Introduction

The study of the polarization of starlight is a relatively new facet to astrophysics. The fact that starlight can be polarized in general was discovered independently and simultaneously in 1948 by Hall (1949) and Hiltner (1949a). At the time of the announcement of the discovery, although the investigation was related to polarization engendered within stellar atmospheres (intrinsic effects), it was immediately apparent that the polarization was produced in the interstellar medium by the passage of the light through dust clouds. Since then observational polarization studies have become more diverse with later discoveries related to intrinsic effects within stellar atmospheres which triggered off the original research. However, knowledge of interstellar polarization here is still important so that its contamination can be subtracted, allowing proper modelling of the intrinsic effects.

It can be fairly stated that much of our knowledge of the properties of interstellar dust grains and their distribution in the galaxy comes from polarization measurements in association with spectrophotometric data. The first measurements of polarization involved the linear form but more recently, with improved techniques, circular polarization is now included in the study.

The theme of this thesis will concentrate on two aspects of interstellar polarization, *viz.*

- (i) The general form of the wavelength dependence,
- (ii) The behaviour of the form in complex cloud situations.

Under (i) we shall investigate the way in which the deduced parameters describing the wavelength dependence may be affected by noisy data and under (ii) we shall look at the behaviour of the wavelength

dependence of polarization in the two-dust-clouds situation, i.e. in circumstances where dispersion of the position angle is evident.

1.2 Interstellar Polarization

Prior to the discovery of interstellar effects there had been a few specialised stellar polarimetric investigations; a noteworthy example is Babcock's (1947) investigations of stellar magnetic fields through the Zeeman effect and its associated polarization. A great impetus occurred through the theoretical work of Chandrasekhar (1946) on radiative transfer. His analysis predicted that for early-type stars, in which the electron scattering is the source of opacity, 12 percent of the light emanating from a given point at the stellar limb might be plane polarized, with the electric vector parallel to the limb. This polarization might be detected in a binary situation when the early-type component is occulted by the late-type companion.

The investigations carried out independently by Hall (1949) and Hiltner (1949a) were directed to look for the effect predicted by Chandrasekhar, but instead their investigations led to the discovery that the light of the majority of distant stars is generally partially plane polarized; the degree of polarization is well correlated with distance modulus and interstellar absorption lines or bands so indicating an interstellar origin. These studies introduced a new means of investigating the interstellar medium.

Large numbers of stars, mainly O and B type, have now been observed for this effect (see for example Hiltner (1951a, 1954a, d, 1956)). From such measurements the galactic structure dependence of polarization can be investigated. All the data show that the amount of polarization decreases rapidly with increasing galactic latitude. The galactic longitude dependence of polarization for stars further than

several hundred parsecs may be represented by a double sine wave with minima at galactic longitudes 50° and 230° (Hall and Serkowski (1963)), which are approximately the directions of galactic spiral arms as determined by Morgan, Whitford and Code (1953). More recently all the available data on the interstellar linear polarization have been compiled by Mathewson and Ford (1970). More than 7000 stars are included in both northern and southern hemispheres, with the direction and magnitude of the polarization plotted on a map with galactic co-ordinates as shown in Fig. 1.1. This work and its developments still remains paramount, for example in searching for regions with systematic polarization alignment or the variation of the degree of alignment with galactic longitude. A well defined region with the degree of alignment parallel to the galactic plane is found at about 130° longitude which is interpreted as due to looking across a spiral arm. On the other hand the random alignment seen near 80° longitude has been interpreted as due to viewing along the magnetic lines of force in a spiral arm but Verschuur (1974) suggests that this random alignment is due to a local disturbance associated with the Cygnus X-1 source.

1.3 Wavelength Dependence of Interstellar Polarization

Investigations to see whether there is any wavelength dependence of interstellar polarization, $p(\lambda)$, commenced in the late 1950's when Behr (1959a) made observations of seven stars using three bands at wavelengths $\lambda\lambda$ 3710, 4300 and 5160. He found that for all the observed stars, except α Cyg, the polarization in the ultraviolet is slightly smaller than in the blue and for some stars the polarization in the yellow is smaller than in the blue while for others it was larger. The polarization variability for the star γ Cas was also observed by Behr (1959b) which is direct evidence for intrinsic polarization (an aspect which will be considered later in this chapter). By extending the

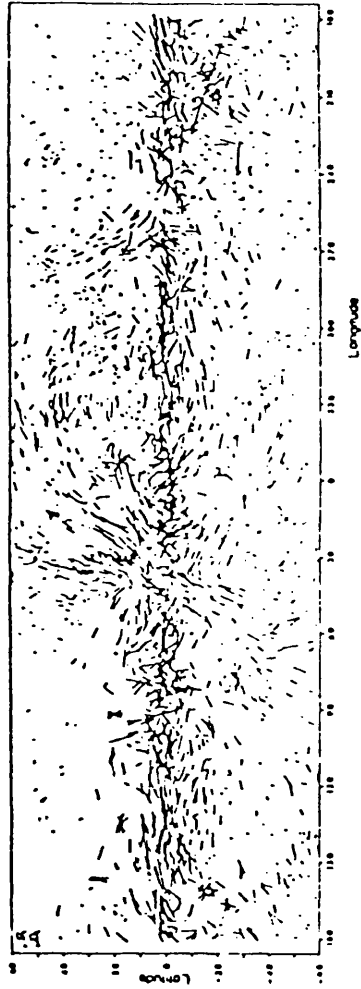


Fig. 1.1 The interstellar polarization of starlight plotted in galactic co-ordinates. (Ref. F1.1)

wavelength coverage, Gehrels (1960) obtained a remarkable curve for $p(\lambda)$ from an average of eight stars; the curve had a flat maximum near $\lambda = 6500 \text{ \AA}$, decreasing sharply towards longer and gradually towards shorter wavelengths as shown in Fig. 1.2. (N.B. p is plotted against $1/\lambda$).

Subsequent to the discovery of $p(\lambda)$, it had been realised that under certain conditions one should find a dependence of the position angle of the polarization on wavelength (see Serkowski (1962) and Treanor (1963)). Treanor's prediction was: "If the existence of a colour dependence of polarization on particle size is accepted, physical situations will undoubtedly arise in which this will entail also a colour-orientation dependence. The most easily envisaged case is one in which starlight passes through two successive clouds with different orientation of the dust particles relative to the line of sight and different mean projected particle size." The evidence associated with this prediction was first detected by Gehrels and Silvester (1965). More detailed discussions on this effect are deferred to Chapter 4.

As a continuation of the study, the wavelength dependence theme was extended by Coyne and Gehrels (1966) through a survey of eighteen stars over a broad range of wavelengths ($0.3 - 1.0\mu$). The general form of the $p(\lambda)$ curve was observed and later confirmed by another survey made for thirty-three O and B type stars (Coyne and Gehrels (1967)).

The survey was later extended to the southern hemisphere and observations were made by Serkowski and Robertson (1969) in the UBV bands (p_U, p_B, p_V) for stars with large interstellar linear polarizations to study the distribution on the sky of the ratios such as p_V/p_B .

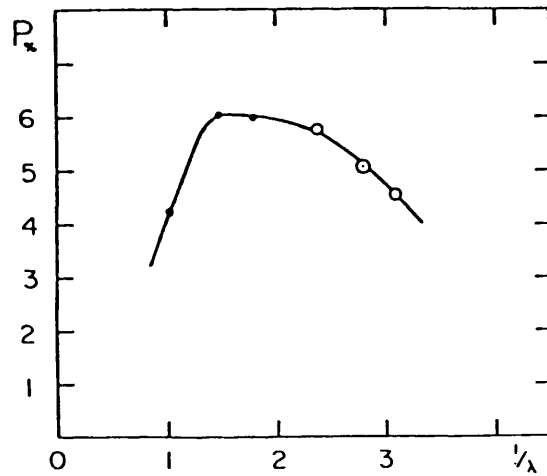


Fig. 1.2 Observed percentage of interstellar polarization as a function of the inverse of the wavelength as observed by Gehrels. (Ref. F1.2)

Well defined regions on the sky are found with the ratio smaller than the median value, which was considered to be 1.055, and others are apparent with a systematic larger ratio. The largest values of the ratio are found in the relatively nearby associations in Orion and in Ophiuchus - Upper Scorpius, and among the more distant stars the only large region with predominantly high values of the ratio occurs at longitude 290° - 345° (including the association I Ara).

Further observations of the wavelength dependence were made by Coyne and Wickramasinghe (1969) for early-type stars in the wavelength range $0.3 - 0.9\mu$ and they produced a grain model to fit the observations. Their best model fit consisted of a thin graphite disk with radius of 0.5μ embedded in a dielectric oblate spheroid with semimajor axis $a = 0.3\mu$ and semiminor axis af with values of f for the best fit given by $0.7 \leq f \leq 0.8$. From all the measurements of $p(\lambda)$ it was found that there was a maximum value for the polarization, p_{\max} , at a particular wavelength, λ_{\max} . A survey was made for all the available data on $p(\lambda)$ by Serkowski, Mathewson and Ford (1975) (afterwards referred to as SMF) to investigate the behaviour of λ_{\max} over the sky. Well defined regions are found with λ_{\max} less than the median value, which was taken to be 0.545μ , and other regions with λ_{\max} larger than this median value as shown in Fig. 1.3 which is based on values for about 350 stars. The largest and best defined region of low λ_{\max} lies along the galactic equator at longitudes 115° - 150° and for high λ_{\max} at longitudes 295° - 350° and it is found that the largest values of λ_{\max} are observed for these relatively nearby stars in Upper Scorpius and Orion which are characterised by a large ratio (R) of total to selective interstellar extinction and also with large p_V/p_B ratio (see Serkowski and Robertson (1969)); the linear size of regions with similar $p(\lambda)$, i.e. with similar average size of dust grains, is about

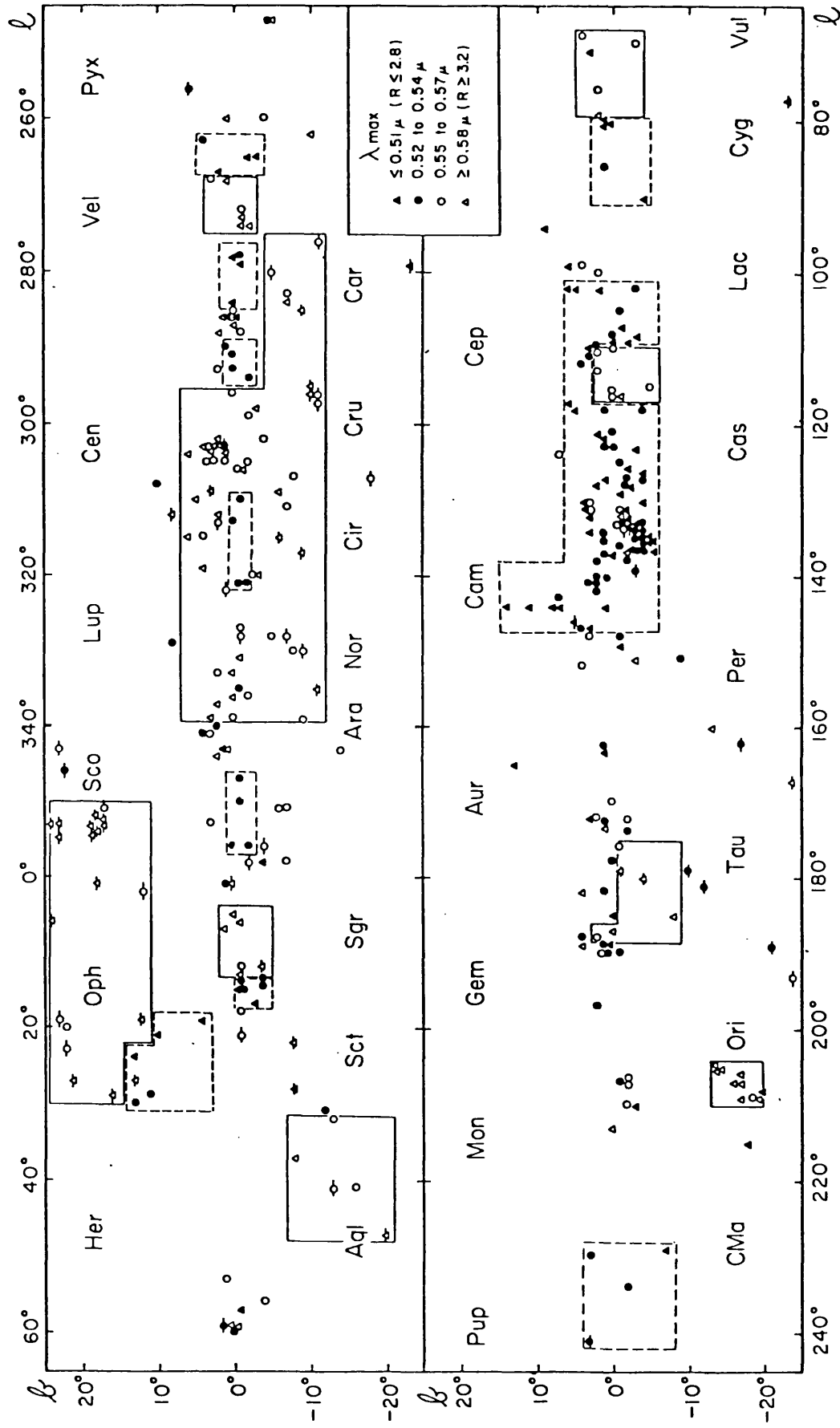


Fig. 1.3 The wavelength of the maximum interstellar polarization, λ_{\max} , plotted in galactic co-ordinates. (Ref. F1.3)

150pc this being approximately the size of large clouds of interstellar medium as derived by Scheffler (1967). The conclusion from this survey was that in general the nearby stars have considerably larger λ_{\max} than the stars more distant than 0.4 kpc. This can be explained on the basis of a selection effect whereby the closer stars, for which polarization is so large that λ_{\max} can be determined easily, are often seen through a relatively dense dust cloud and it was shown by Carrasco, Strom and Strom (1973) that the size of dust grains and λ_{\max} seem to be larger in the more dense dust clouds.

Serkowski (1973) noticed that the shape of the wavelength dependence of interstellar polarization seems to be the same for all stars when it is normalised. By plotting the ratio $p_{\lambda}/p_{\lambda_{\max}}$ against the ratio λ/λ_{\max} for all stars, a single curve results which is well described by the empirical formula:

$$P_{\lambda}/P_{\max} = \exp[-K \ln^2(\lambda_{\max}/\lambda)] \dots\dots\dots 1.1$$

where $K = 1.15$ for the best fit. This relationship is referred to as "Serkowski's Law".

By comparing models for the interstellar grains Coyne, Gehrels and Serkowski (1974) (afterwards referred to as CGS) found that the best fit to the observations of $p(\lambda)$ is provided by dielectric cylinders of constant "elongation", e , where $e = \frac{b}{a}$, a = radius of cylinder and b = length, having a size distribution similar to the Oort - Van de Hulst distribution, with refractive index $m = 1.33$ and oriented by the Davis - Greenstain Mechanism (see Shah (1967), Fig. 50, Greenberg (1968) Fig. 95). This model fit coincides almost perfectly with the empirical curve presented as Equation 1.1. Figures 1.4, 1.5, 1.6 represent the normalised values for $p(\lambda)$ for all stars observed in Arizona (CGS), in Australia (SMF), and for all multicolour polarimetric

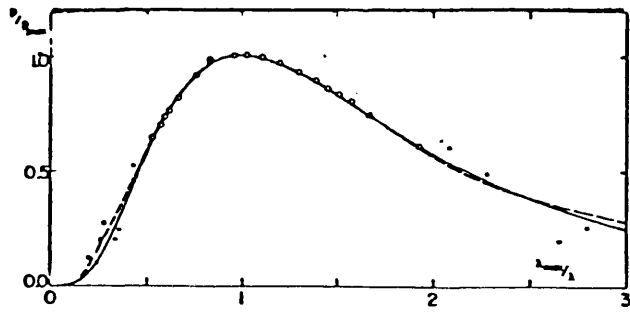


Fig. 1.4 The normalised wavelength dependence of interstellar linear polarization for stars observed with the Wollaston polarimeter at University of Arizona. (Ref. F1.4)

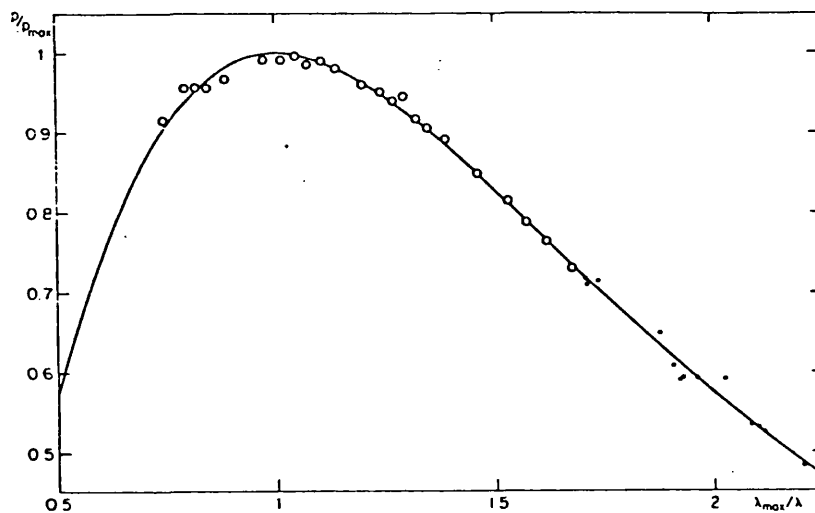


Fig. 1.5 The normalised wavelength dependence of interstellar linear polarization for stars observed with the Siding Spring polarimeter. (Ref. F1.5)

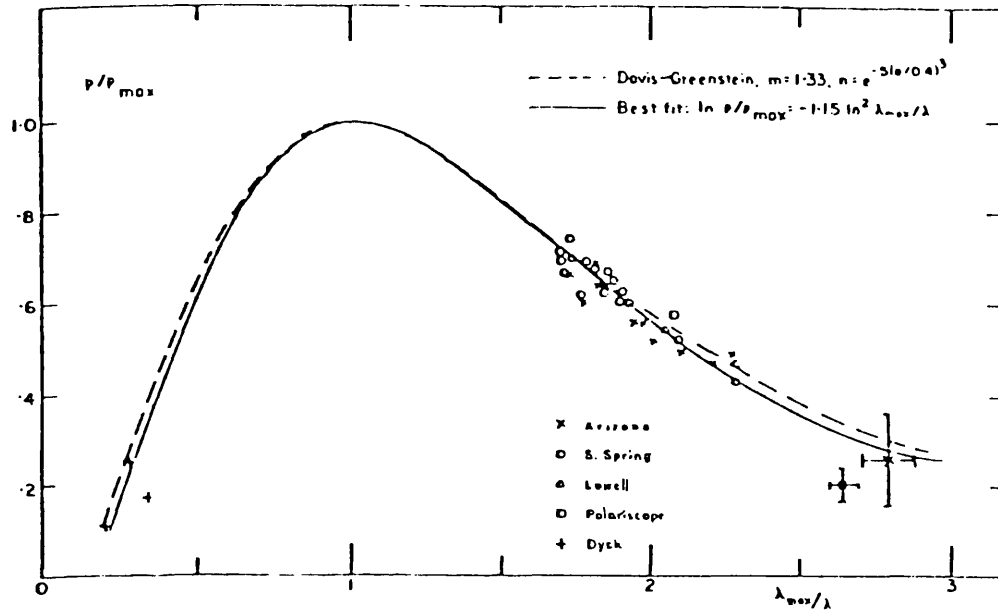


Fig. 1.6 The normalised wavelength dependence of interstellar linear polarization for all multicolour polarimetric observations compared with a theoretical model. (Ref. F1.6)

observations respectively, compared with Equation 1.1 and the theoretical curves. Fig. 1.6 also includes some observations at the extreme value of λ_{\max}/λ to show the scatter which exists among various stars. The pronounced correlations between λ_{\max} and colour excesses have been investigated (cf. Serkowski 1968, 1973) leading to the conclusion that λ_{\max} is proportional to the average size of interstellar dust grains which produce both the extinction and polarization. The relationship between p_{\max} (%) and the colour excess E_{B-V} is shown in Fig. 1.7; the ratio $P_{\lambda_{\max}}/E_{B-V}$ rarely exceeds the value of 9.0 which is represented by the straight line in the figure, the ratio for each star being taken as the measure of alignment of the interstellar dust grains by the galactic magnetic field.

It has been shown also by Serkowski (1973) and SMF that there is a correlation between variations in λ_{\max} and variations in the extinction law for various regions of the galaxy. By normalising the wavelength scale of the extinction using respective values of λ_{\max} for the Perseus - Cepheus and Scorpius regions of the galaxy, the two curves coincide as shown in Fig. 1.8, which is adapted from Serkowski (1973). The interpretation of these curves as indicated by Coyne (1974a) is that both variations in λ_{\max} and in the extinction curves reflect variations in the mean size of the interstellar particles for different regions. In addition Coyne suggested that λ_{\max} is expected to be proportional to the mean value of $(m - 1)r$, where m is the index of refraction and r is the mean particle radius, and the normalisation of the extinction curves assumes that m is approximately constant with wavelength. Therefore the normalisation will not work in spectral regions where the extinction is dominated by a strong absorption feature, as is the case in the far ultraviolet where the wavelength dependence of extinction is dominated by a strong absorption feature around 0.22μ (Bless and Savage (1972)).

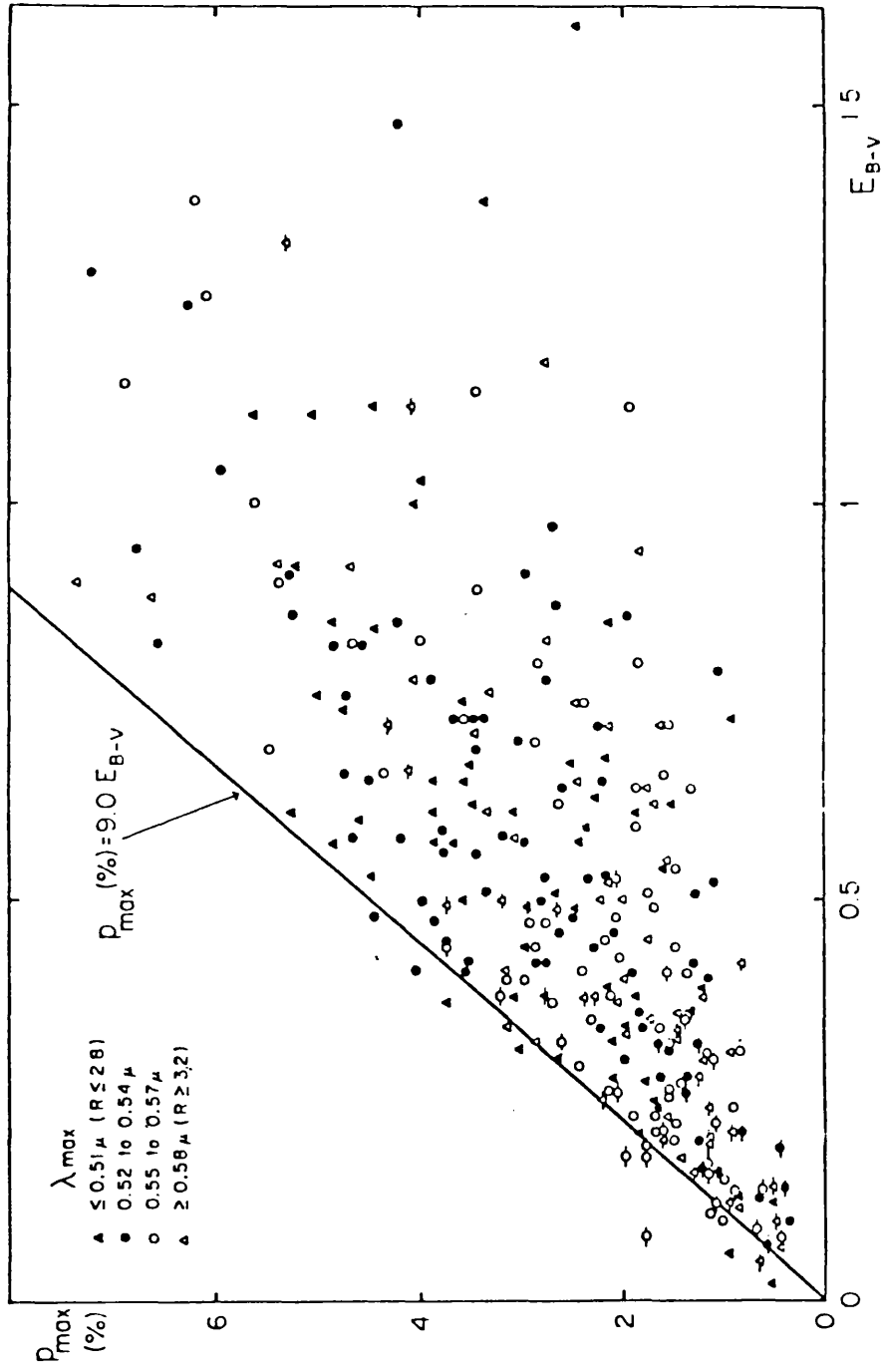


Fig. 1.7 The relationship between the maximum interstellar polarization P_{\max} (%) and colour excess E_{B-V} . (Ref. F1.7)

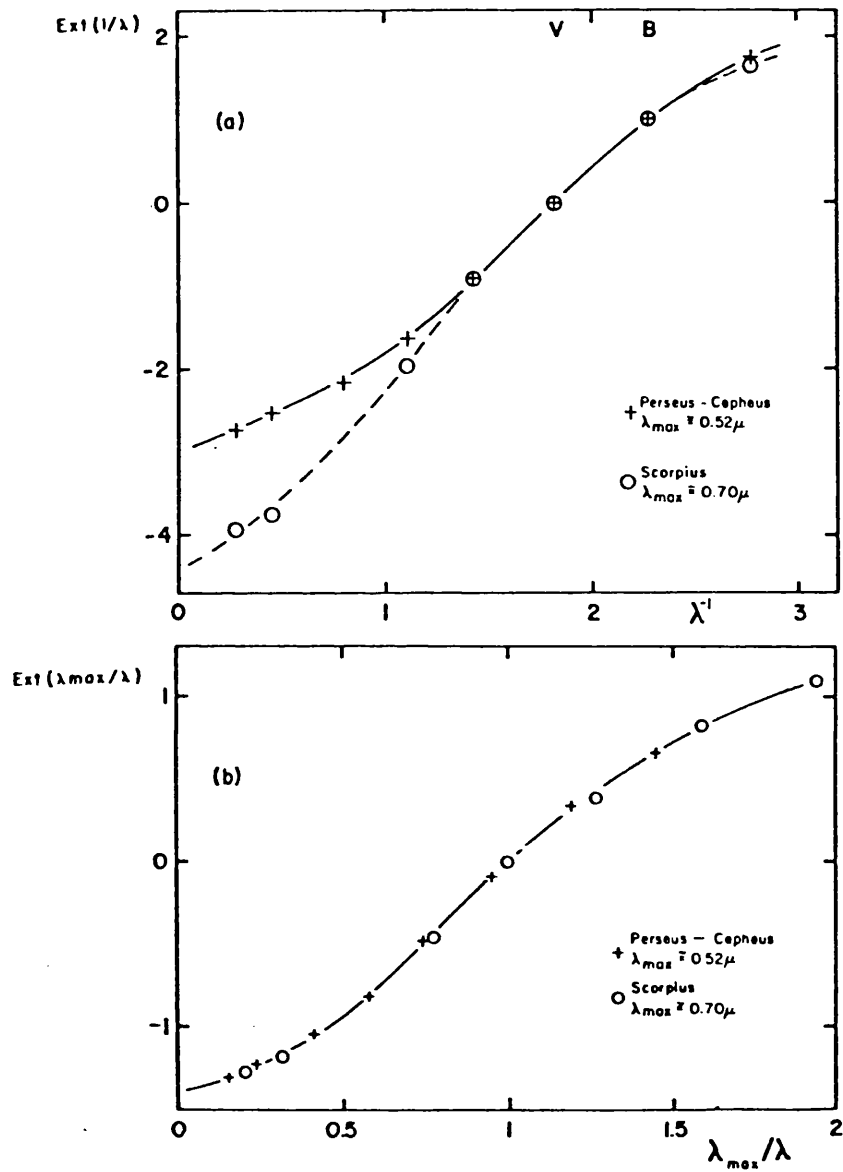


Fig. 1.8 Wavelength dependence of interstellar extinction for the stars in Perseus-Cepheus and in Scorpius.
 a. The traditional extinction curves.
 b. The extinction curves normalised to λ_{max} , the wavelength of maximum polarization.
 (Ref. F1.8)

In the early stages of the investigations into the nature of the dust grains many different materials have been suggested as constituents of the interstellar medium. This is because the free parameters defining the size distribution were sufficient to explain the observations in the wavelength region from near infrared to near ultraviolet (Greenberg (1978)), but with extended observations in the far infrared and the far ultraviolet the situation has become clearer. Essentially the materials which have been proposed fall into two main categories. These are dielectrics (ices and silicates) and metallics (graphite and magnetite).

It can be fairly stated that some restrictions on the type of grain material have been placed through the analysis of the observations of interstellar linear polarization. For instance the dielectric grains (ices), which are characterised by their refractive index being constant (real) in the visible range of wavelengths, have been widely considered to be sufficient to interpret the normalised curve of $p(\lambda)$ (see CGS).

Interstellar polarization study has been developed by the discovery of circular polarization (see Martin, Illing and Angel (1972)). The wavelength dependence of circular polarization in a number of different regions on the sky shows that the polarization changes sign at a wavelength (λ_c) almost equal to the wavelength of the maximum linear polarization (λ_{max}). A correlation between λ_c and λ_{max} should be expected as the same grains cause both linear and circular polarization. The ratio λ_c/λ_{max} is now considered to be a new tool to investigate further the nature of dust grains (Martin (1972)). All the measurements reveal that the ratio $\lambda_c/\lambda_{max} \approx 1$, while the theoretical study shows that this ratio approaches unity as the imaginary part of the refractive index goes to zero - i.e. for pure dielectric

materials the ratio $\lambda_c / \lambda_{\max} = 1$. So with circular polarization observations restriction on grain composition can be obtained but without providing an unique identification. Further restrictions should be possible by extending circular polarization measurements into the infrared and ultraviolet.

Polarization measurements have also been applied to several associations and clusters and these have been reviewed recently. McMillan and Tapia (1977) made measurements of $p(\lambda)$ for members of the Cyg OB2 association obtaining the standard $p(\lambda)$ curve; λ_{\max} agreed with the normal extinction law in the region of the association. An improved value of the position angles for the association was obtained after the subtraction of an assumed uniform foreground polarization with the relevant values for λ_{\max} , p_{\max} and position angle. Coyne, Tapia and Vrba (1979) made measurements for a large number of stars assumed to be members of the α Per star cluster (a group of about 200 stars in the spectral range B7 - B9) and of surrounding stars, but not cluster members, in order to determine $p(\lambda)$ in and about the cluster. From the obtained values of λ_{\max} they concluded that the dust grains in the cluster have the same mean size and the same mean size dispersion as the grains of the average interstellar medium. The data of this study have been combined with all the previously published data on this cluster (see Kruszewski (1963), Appenzeller (1971) and Markannen (1971)) in order to make better estimates for the parameters characterising the cluster, such as its size, mass, distance, etc. From these parameters they concluded that a magnetic field of about 1×10^{-4} G is necessary to produce the observed polarization.

Challenges to the general universality of Serkowski's Law (Eq. 1.1) have been made recently. Codina-Landaberry and Magalhães (1976) suggest

that K may vary from star to star; a value of $K = 1.15$ gives the best fit for the set of stars considered as a whole but it does not yield the best representation of the wavelength dependence for each treated separately. Their approach has been to compute λ_{\max} , P_{\max} and K where K was allowed to be a free parameter for each star. A range of values of K were obtained implying differences in the shape of the $p(\lambda)$ curves. Figures (1.9) and (1.10) represent the curves for two stars with the values of $K = 0.19$, $K = 1.47$ respectively. The figures include also the observational and theoretical curves based on the value of $K = 1.15$. They conclude that for some stars, the dust size varies along the line of sight with changes in alignment so affecting the value of K . Their interpretation is perhaps premature in that the star sample is small and no reference is made to the range of values of K for a control set of stars in the simple cloud situation.

Another defect of the universality of Serkowski's Law seems to appear in the infrared. Recently Dyck and Jones (1978) have applied spectropolarimetry in the infrared to seven stars. They found that their extended measurements did not match the extrapolation of optical band measurements which had been fitted to Serkowski's Law with $K = 1.15$, with the polarization tending to decrease much less rapidly at wavelengths longward of λ_{\max} than predicted by the formula.

Infrared measurements have been pursued by Wilking, Lebofsky, Martin, Rieke and Kemp (1980) (afterwards referred to as WLMRK). Measurements have been made for 24 stars and by combining these with previous optical data they confirmed the observations by Dyck and Jones that infrared values do not match values predicted by the Serkowski formula as fitted to optical data. In applying the Serkowski Law to their complete data for optical and infrared wave-

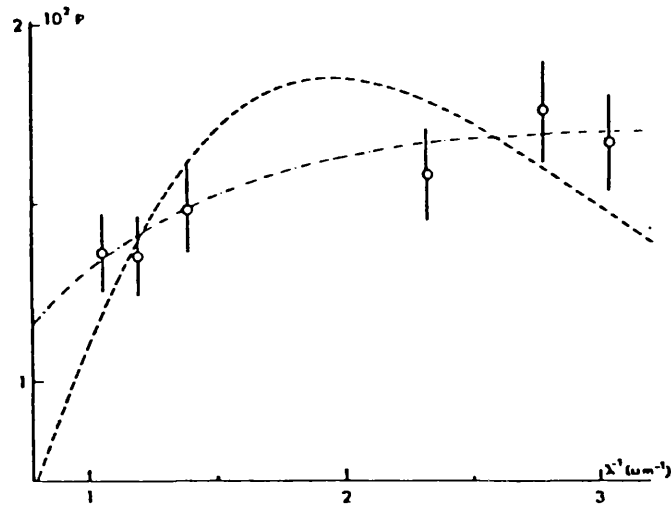


Fig. 1.9 Wavelength dependence of linear polarization of HD 22253 compared with Serkowski's Law for $K = 1.15$ and $K = 0.19$. (Ref. Fl.9)

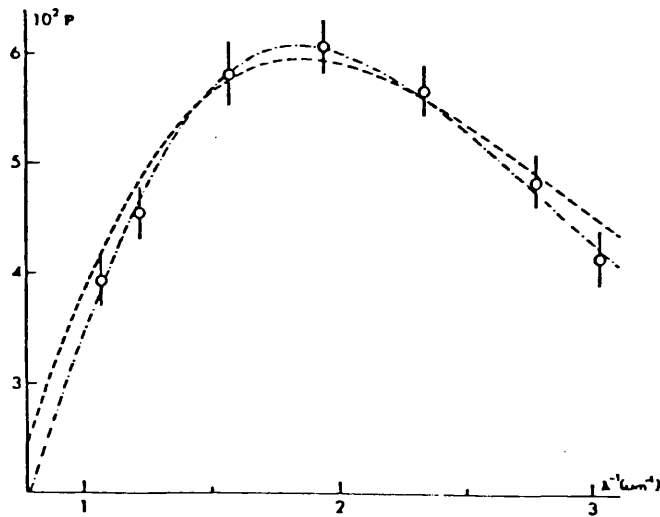


Fig. 1.10 Wavelength dependence of linear polarization of HD 183143 compared with the calculated curves for $K = 1.15$ and $K = 1.47$. (Ref. 1.10)

lengths, they allowed K to be a free parameter and claim that by doing this p_{\max} and λ_{\max} are better defined particularly for cases where λ_{\max} lies at near infrared wavelengths. They conclude that there is a strong correlation between λ_{\max} and K , as shown in Fig. 1.11, with the normalised polarization curve apparently narrowing as λ_{\max} increases. They have quantified the relationship by modifying the Serkowski Law to:

$$\frac{p(\lambda)}{p_{\lambda_{\max}}} = \exp[-1.7 \lambda_{\max} \ln^2(\frac{\lambda_{\max}}{\lambda})] \quad \dots\dots\dots 1.2$$

The drawn line in the figure represents the least squares best fit (the stars with rotation of position angle were excluded) and is defined by:

$$K = (-0.002 \pm 0.07) + (1.68 \pm 0.013)\lambda_{\max} \quad \dots\dots\dots 1.3$$

According to the revised formula of Serkowski's Law the broadening of the $p(\lambda)$ curve is now associated with decreasing λ_{\max} values. The shape of the curve according to the authors is related to the physical properties of the interstellar grains; a narrowing of the curve may reflect a narrowing of the size distribution of the grains or an increasing of the real part of the refractive index or the grain shape becoming more spherical.

It is the aim of the first part of this thesis (Chapter 2) to investigate further the nature of this correlation between K and λ_{\max} , with discussions based on the mathematical behaviour of the law rather than on its astrophysical interpretation.

1.4 Intrinsic Polarization

As was mentioned earlier in this discussion, the first detection of intrinsic polarization was reported by Behr (1959b) who observed

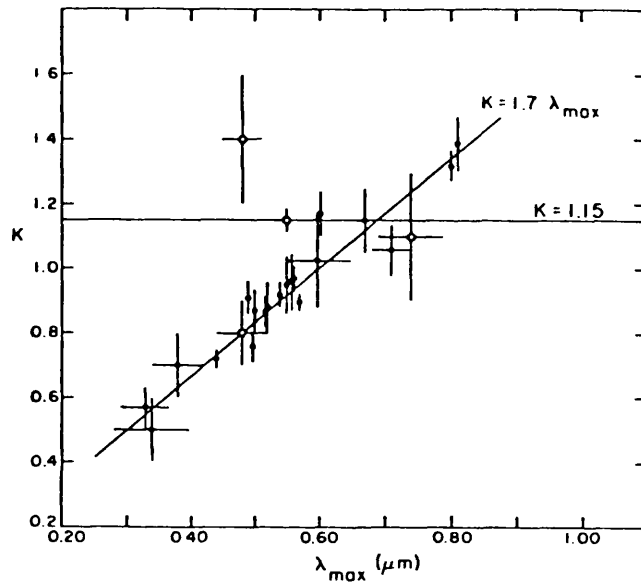


Fig. 1.11 A plot of K against λ_{\max} for 24 stars by WLMRK. (Ref. F1.11)

the polarization variability of the early-type star γ Cas, so opening up a new avenue of astrophysical research. Polarization variability studies have been expanded by the discovery of the intrinsic polarization associated with the eclipsing binary star β Lyr by Shakovskoj (1962a, 1964). This has been confirmed by Appenzeller (1965) and Serkowski (1965) and other eclipsing binaries are now known to display intrinsic effects.

Coyne and Gehrels (1967) have observed the intrinsic variability effect for seven objects from their survey of 33 stars. Four are spectroscopic binaries, e.g. ϕ Per with a period of 127 days, showing variation in polarization of the order of $0.2\% \pm 0.02\%$ occurring over a similar period; furthermore this star exhibits a rotation of the position angle with wavelength of the order of 30° .

It is now found that nearly all stars showing emission lines in their spectra, such as Be stars and shell stars, exhibit intrinsic polarization (see Coyne and Kruszewski (1969)). Theoretical studies of Be stars by the above authors suggest that the observed wavelength dependence of these stars is due to a combination of electron scattering, hydrogen absorption and hydrogen emission in the circumstellar envelopes. This suggestion has been supported by Capps, Coyne and Dyck (1973) in their observations of the Be-shell star ζ Tau. Polarization observations of such stars provide constraints for the models of the stars and are useful to the physical understanding of circumstellar envelopes, e.g. their electron densities and temperatures. The rotation of position angle with wavelength, $\theta(\lambda)$, characterises the presence of intrinsic polarization in combination with interstellar polarization (Poeckert (1975), Coyne (1974b)). Detailed analysis of $\theta(\lambda)$ allows the two polarizations to be separated (Coyne and McLean (1975)).

Other characteristics have been observed which are associated with intrinsic polarization and are considered as indicators for intrinsic effects in addition to those outlined above. McLean and Clarke (1979) have summarised the characteristics as follows:

1. Variability of the observed polarization (p , θ) with time.
2. A wavelength dependence of the degree of polarization $p(\lambda)$ very different from that for pure interstellar scattering.
3. Variation of polarization position angle with wavelength, $\theta(\lambda)$, since this is not normally expected from simple interstellar clouds.
4. Changes in the observed polarization (p , θ) across discrete spectral emission or absorption features of stellar origin.

As suggested by the authors, the most common feature associated with intrinsic polarization is its time variability.

Fig. 1.12 (taken from Coyne and McLean (1975)) shows the wavelength dependence of the normalised curve of intrinsic polarization for the star ϕ Per compared with the theoretical model of Capps, Coyne and Dyck (1973).

Such a review of intrinsic polarization and its characteristics is useful even though the remainder of the work in this thesis deals with interstellar polarization. Generally for any study of interstellar polarization of starlight one should consider the possibility that intrinsic effects might be present in the sources. In the remainder of this thesis it can be assumed that every effort has been made to exclude any intrinsic effects present among the data of interstellar polarization.

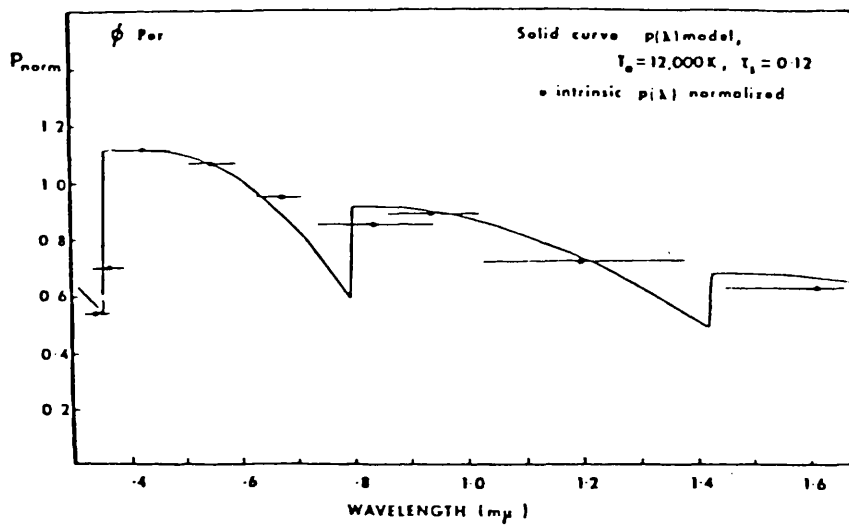


Fig. 1.12 Wavelength dependence of the normalised intrinsic polarization of ϕ Per compared with the theoretical model of Capps, Coyne and Dyck (1973). (Ref. F1.12)

CHAPTER 2

REASSESSMENT OF THE INTERSTELLAR POLARIZATION LAW

2.1 Introduction

2.2 Analysis of the Data

2.1 Introduction

Interstellar polarization provides supplementary evidence to extinction that the light from stars is affected by interstellar grains. An important requirement to produce the polarization is that the grains must be elongated to some degree and that there must be some alignment mechanism, the most favoured at present being paramagnetic relaxation as proposed by Davis and Greenstein (1951). In principle, polarization studies can provide information about the properties of the grains such as their size, shape, refractive index, etc. In addition they also allow investigations of the galactic magnetic field and galactic structure.

The analytic formula for the linear polarization (Serkowski's Law, see Eq. 1.1) has been a landmark in the development of polarization studies. It provides a good fit to observations within the wavelength range ($0.3\mu - 1.0\mu$) and has been proved to be a useful tool in the reduction and interpretation of observations of $p(\lambda)$ for stars with widely differing values of λ_{\max} ($0.4\mu - 0.8\mu$) and differing values of p_{\max} . In addition the parameters which characterise the Law (p_{\max} , λ_{\max} , K) have been related to the properties of the dust grains. The observations of the variability of λ_{\max} , for instance, from one star to another are related to studies of grain size and composition in the galaxy, the efficiency of the alignment mechanism as a function of grain size and the geometry of the alignment, and these are in turn important for studies of the nature and evaluation of the interstellar medium (see Carrasco, Strom and Strom (1973) and Martin (1974)).

More recently, as mentioned in Chapter 1, the universality and exactness of the Law has been questioned (see Codina-Landaberry and Magalhães (1976) and WLMRK), and a correlation is found by WLMRK

between λ_{\max} and the constant K for combined data (optical and infrared) represented by:

$$K = 1.7 \lambda_{\max} ,$$

putting the Law in a new form (see Eq. 1.2). The following section describes the procedure of the analysis for further investigations of this new correlation with the optical data of polarization from existing catalogued measurements.

2.2 Analysis of the Data

Since the discovery of the wavelength dependence of interstellar linear polarization (see Gehrels (1960)), two groups of workers have carried out systematic investigations with measurements over the optical range of wavelengths. As a result of their studies two catalogues have emerged. The first one provides data for stars, mostly in the southern hemisphere, measured in four colours UBVR (see SMF) while the second catalogue provides data for stars, mostly in the northern hemisphere, measured with filters within the range of wavelengths $0.3\mu - 1.0\mu$ (see CGS) [the seven-colour measurements will be considered here]. In order to investigate any possible correlation between K and λ_{\max} for SMF and CGS data, it is necessary to make a reappraisal of the data.

We first deal with SMF data. Although it is not expected that accurate values of K would ensue from four colours only, it was thought that from a large number of stars, any correlation between K and λ_{\max} might still be detectable.

The data tables presented by SMF do not provide the individual values of K directly so the basic measurements which are presented in Table 3 of that paper were used in the calculations.

Not all the stars in the catalogue have been considered and selection was found to be necessary. Only stars with complete four-colour (UBVR) polarimetric data and (B - V) colour index values (so allowing the effective wavelengths of BVR to be determined) were used; those stars which have been designated by SMF as displaying intrinsic polarization or dispersion of the azimuth of vibration were rejected. (Their Fig. 10 summarises this latter group of stars and is reproduced in Chapter 4 as Fig. 4.1). Moreover the data in their Table 3 represent the measurements for each star on different nights but do not provide the individual errors, so that the mean was calculated for each star without weighting. There may, therefore, be slightly different values used in this study from those originally used by SMF but systematic differences are not expected. The effective wavelength for the U-band was taken to be constant as (U - B) data were not available; on the other hand the effective wavelengths for BVR bands for each star were calculated according to the following formula given by SMF:

$$\lambda^{-1}_{\text{eff}} = \lambda_0^{-1} - (B - V)K_B$$

where $K_B = 0.06, 0.025, 0.012$, $\lambda_0^{-1} = 2.23, 1.86, 1.44$ for BVR respectively (see Table 4 of their paper).

The method of the least squares solution which minimises the sum of the squares of the residuals of the measurements, so providing the best values for p_{max} , λ_{max} and K , has been used to refit the data to Serkowski's Law. In allowing K to be a free parameter, limits were set so that its values were within the range (0.2 - 1.7). The following is an outline of the procedure of the method.

The formula for Serkowski's Law is:

$$\frac{P}{P_{\max}} = \exp\left[-K \ln^2\left(\frac{\lambda_{\max}}{\lambda}\right)\right] \dots\dots\dots 2.1$$

(According to Serkowski's original work $K = 1.15$ for all the stars).

By taking the natural logarithm of both sides of Equation 2.1 we obtain:

$$\begin{aligned} \ln p &= \ln p_{\max} - K(\ln \lambda_{\max} - \ln \lambda)^2 \\ \ln p &= \ln p_{\max} - K \ln^2 \lambda_{\max} + 2K \ln \lambda_{\max} \ln \lambda - K \ln^2 \lambda \\ \ln p + K \ln^2 \lambda &= X_1 + X_2 \ln \lambda \dots\dots\dots 2.2 \end{aligned}$$

where

$$X_1 = \ln p_{\max} - K \ln^2 \lambda_{\max} \dots\dots\dots 2.3$$

$$X_2 = 2K \ln \lambda_{\max} \dots\dots\dots 2.4$$

Equation 2.2 was solved for each star by least squares for the unknowns X_1 and X_2 using the above range for $K(0.2 - 1.7)$ and then the values of p_{\max} , λ_{\max} were determined from Equations 2.3 and 2.4.

The number of stars available for analysis following the application of all the criteria described above was 107 (the values of K and λ_{\max} are summarised in Appendix 1). Fig. 2.1 presents the λ_{\max} , K values for these stars. Without more specific analysis at this stage, it is impossible to comment on how much the spread in the values is due directly to the noise on the polarimetric measurements and how much it is due to a natural dispersion caused by differing interstellar conditions along the line of sight to each star. Evaluation of the mean value of K gives approximately 1.15 as obtained by SMF and since used by many workers in the field.

The full line with negative slope corresponds to the least squares solution of the best straight line and is expressed by:

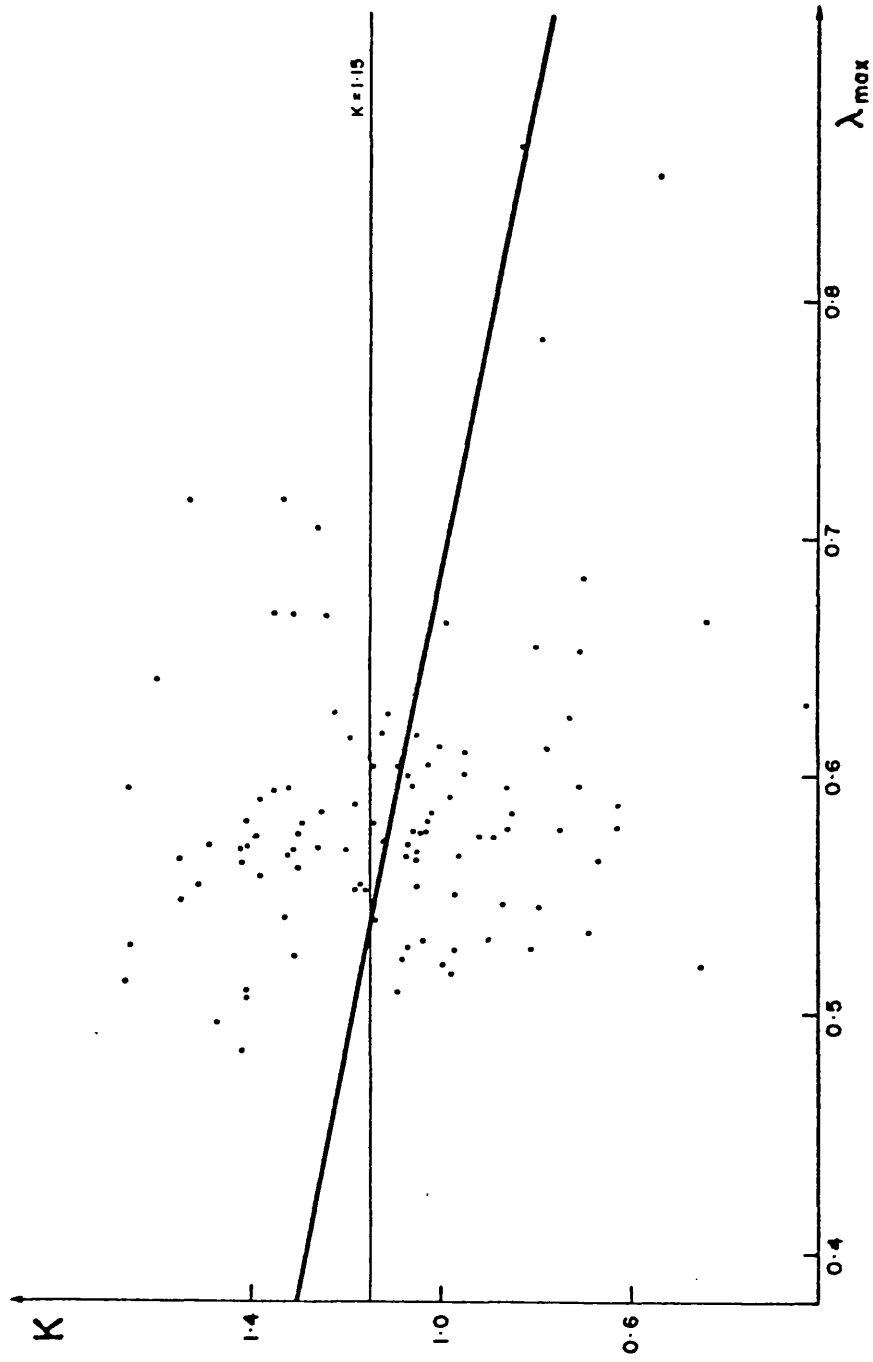


Fig. 2.1 The correlation between K and λ_{\max} for 107 stars from SMF

$$K = 1.186 - 1.002(\lambda_{\max} - 0.5) \dots\dots\dots 2.5$$

This correlation (later shown to be significant) appears to have been overlooked by Serkowski and associated workers. More importantly, the form of the correlation is significantly different from that obtained by WLMRK (1980) which shows an opposite sense of the slope (see Fig. 1.11).

In order to test the significance of the negative slope evaluated above, a statistical procedure, which is described by Young (1962), has been applied to the data. Calculations were performed for the gradients of the least squares fitted line to K as a function of λ_{\max} (the full line) and λ_{\max} as a function of K (the reciprocal of the first gradient), and then taking the square root of their product we get the correlation coefficient. The value obtained is then compared with Table VII (values of the correlation coefficient for different levels of significance), from Fisher and Yates (1963). This exercise indicated that there is an approximately 95% confidence level on there being a correlation between K and λ_{\max} in the form presented above.

In order to investigate further the reason behind this newly discovered correlation, we have considered CGS data as well, covering the wavelength range from approximately 3300 Å to 9500 Å. The basic measurements are not presented in CGS so we referred to the papers listed in the last column of Table II. The data were taken from the following papers: Coyne and Gehrels (1966), Coyne and Gehrels (1967), Coyne and Wickramasinghe (1969), Serkowski, Gehrels and Wisniewski (1969) and Coyne (1974b). (N.B. most of the data presented in these papers are already weighted).

Selection of the stars was based on conditions that they should have accurate polarimetric measurements for seven colour bands. Stars

known to have intrinsic polarization or those listed by Coyne (1974b) as displaying dispersion of the azimuth of vibration were rejected. The same procedure of the least squares solution has been applied to the selected stars and the number of stars now available for correlation analysis is 73. (The values of K and λ_{\max} are summarised in Appendix 2). The values of λ_{\max} and K are displayed in Fig. 2.2 and the full line with positive slope is the least squares solution of the best straight line and is expressed by:

$$K = 1.01 + 2.83(\lambda_{\max} - 0.5) \dots\dots\dots 2.6$$

The form of correlation between K and λ_{\max} obtained from these data is significantly different from the previous one for UBVR bands. From the statistical test, outlined above, the level of confidence for the above correlation is 99.9%, this being strongly significant.

The question immediately arises as to why there is a change in the form of the correlation (from negative to positive) between K and λ_{\max} as the wavelength range is extended. With this in mind and as a check, the data with seven-colour measurements were reduced to four with the chosen colours being closest to the UBVR bands and the same analytical procedure was applied to the data. By this selection 62 stars were available for analysis. (Appendix 2 includes the values of K and λ_{\max} for these stars). The values of λ_{\max} and K for these stars are displayed in Fig. 2.3. The data revert to show a negative slope and the full line is the least squares solution of the best straight line expressed by:

$$K = 1.10 - 1.24(\lambda_{\max} - 0.5) \dots\dots\dots 2.7$$

The above correlation is with 95% confidence which is almost similar to the correlation obtained directly from SMF data depicted in Fig. 2.1.

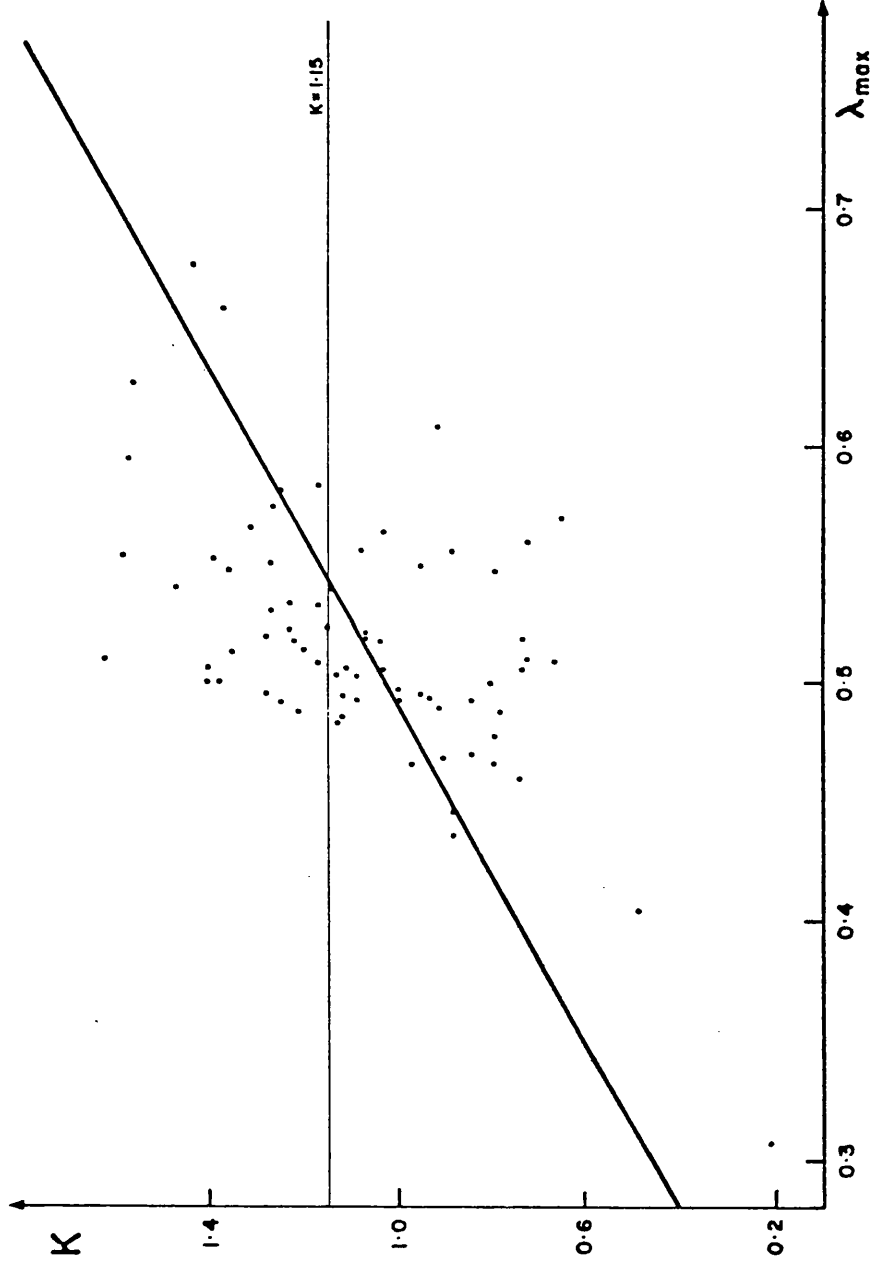


Fig. 2.2 The correlation between K and λ_{\max} for 73 stars measured with seven colours from CGS

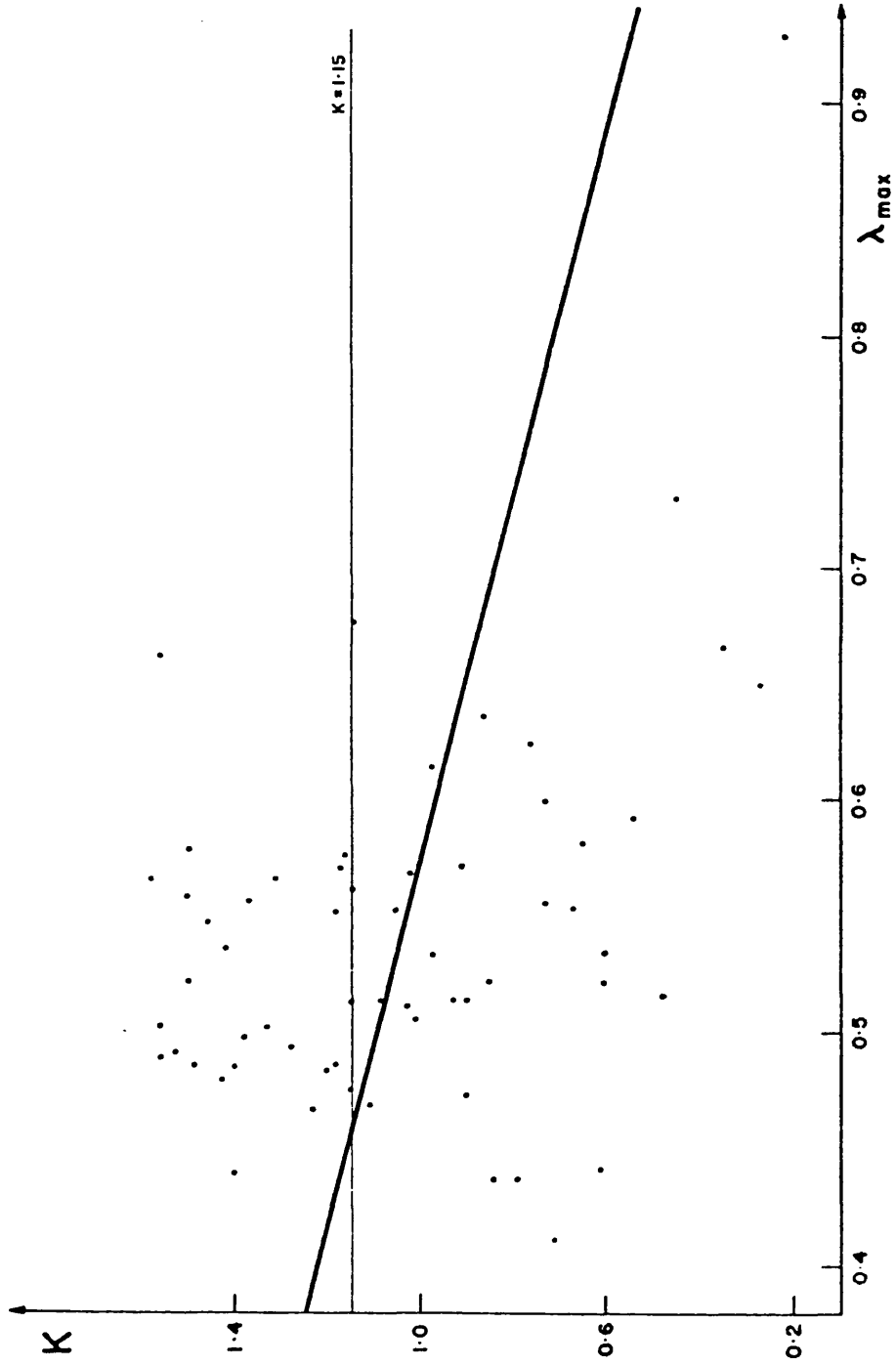


Fig. 2.3 The correlation between K and λ_{\max} for data reduced to four colours for 62 stars from CGS

Comparison between the values of K obtained by using seven wavelengths (K_7) with those values for four wavelengths (K_4) showed a big difference for most of the stars. Fig. 2.4 shows the relationship between K_4 and K_7 ; the full line is the least squares solution of the best straight line expressed by:

$$K_4 = 0.92 + 0.42(K_7 - 0.8) \dots\dots\dots 2.8$$

while the broken line represents the perfect correlation ($K_4 = K_7$).

In a similar way the values of λ_{\max} have been compared for the two sets of data and showed slight differences for most of the stars. These are displayed in Fig. 2.5 with the full line being the best straight line expressed by:

$$\lambda_{\max_4} = 0.52 + 1.05(\lambda_{\max_7} - 0.5) \dots\dots\dots 2.9$$

while the broken line again represents the perfect correlation, the two lines being close.

A group of stars near the Orion Nebula for which the polarization measurements were made by Berger (1977) has also been considered. The basic measurements are represented in Table 1 of the above cited paper. Similar results were obtained by applying the same procedures to the data, i.e. a positive slope (+ 0.96) between K and λ_{\max} ensued when the broadest wavelength coverage was used and again a negative slope (- 0.31) resulted when the data were reduced to four-colour values closest to UBVR.

Such an outcome of the correlation between K and λ_{\max} being dependent on the wavelengths of the data points raises many questions. Might not the new interstellar polarization law proposed by WLMRK (1980) (see Eq. 1.2) be the natural outcome of the choice of a particular filter set and not need any astrophysical arguments to describe its form? The various correlations above might ensue if the form of Serkowski's Law

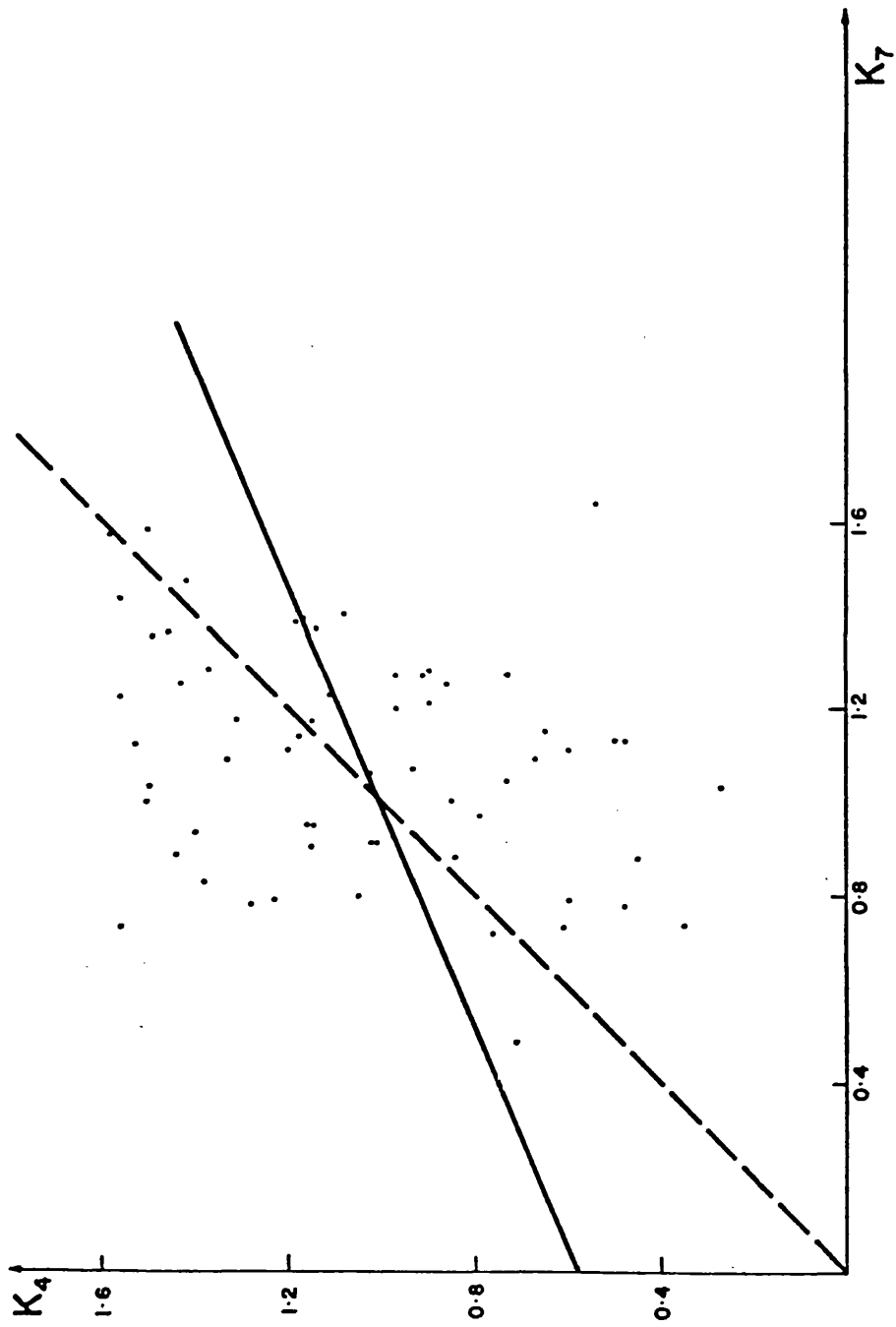


Fig. 2.4 Plots of K values for four-colour measurements against the K values for seven-colour measurements

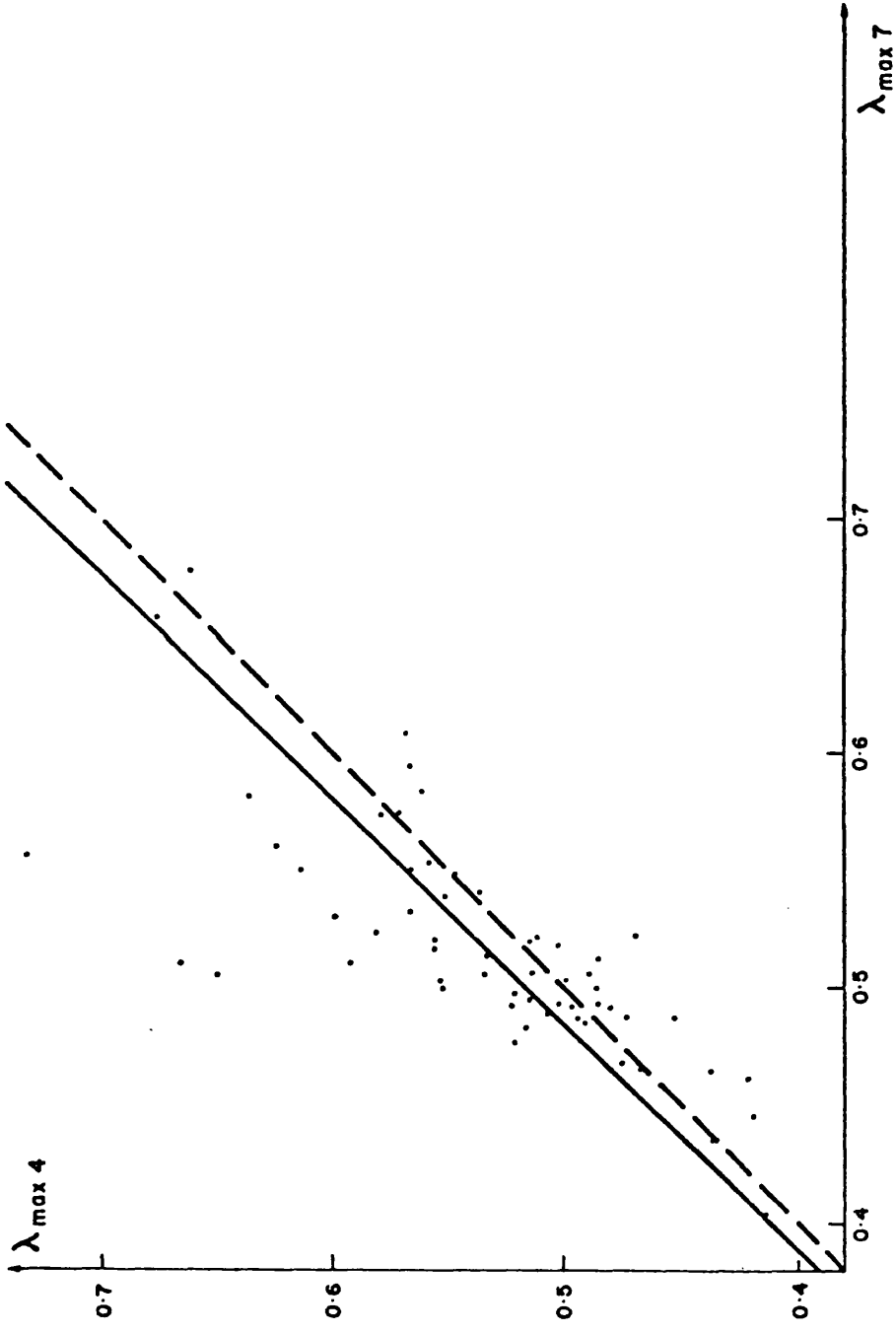


Fig. 2.5 Plots of λ_{\max} values for four-colour measurements against the λ_{\max} values for seven-colour measurements

is not sufficiently good to describe the shape of the normalised interstellar polarization law accurately over wide wavelength ranges, perhaps being dependent also on where λ_{\max} is placed relative to the range.

The figure relating K_4 with K_7 (see Fig. 2.4) shows that the K values are noisy. The parameter K is a very sensitive indicator of the half-width of the $p(\lambda)$ curve. For values of $p(\lambda)$ which carry the usual experimental noise, then we expect the determined values of K to reflect this noise. A question to be investigated is "What value of noise might we expect on K for given noise values on $p(\lambda)$?" In addition, we might also consider the possibility of there being naturally occurring correlated biases between the derived values of parameters such as K and λ_{\max} . For example, since the number of data points on the $p(\lambda)$ curve is low (typically 4 or 7) there is a reasonable chance that, for any one star, the measured values might have deviations which give a positive (or negative) bias to the $p(\lambda)$ curve with respect to the true curve for that star; this of course affects the determined value of K but it may also affect the determined value of λ_{\max} .

Estimates of the expected scatter in the values of K according to noise values on $p(\lambda)$ are difficult to obtain analytically but can easily be assessed by numerical methods.

The following chapter describes the procedures which have been applied to the data to investigate the effects of noise on the determined values of K and λ_{\max} and to investigate the possibility of forced correlations occurring between these parameters and how these depend on the value of λ_{\max} relative to the wavelength range of the data set.

CHAPTER 3

A NUMERICAL INVESTIGATION OF NOISY POLARIMETRIC DATA

3.1 The Computer Programme Scheme

3.2 Analysis of Simulated Noisy Data

3.1 The Computer Programme Scheme

With the notion that noisy data by their nature might provide correlations between the characteristic parameters of the interstellar polarization law, K and λ_{\max} , a computer programme was written to investigate the idea. The following is a description of the scheme whereby artificial data (with noise) are generated and then analysed by fitting them to the Serkowski Law.

For convenience, it is assumed that the Serkowski Law with the value of $K = 1.15$ is the true representation of the situation (any other chosen value of K or even the use of the newly proposed law of WLMRK for this exercise would not alter the generalities of the conclusions here). The computer programme allows the choice of p_{\max} and λ_{\max} and the selection of wavelength values corresponding to filter sets so that any measurement situation can be reproduced. A value for the amplitude of a random noise function can also be set. When the programme is run, the perfect values of $p(\lambda)$ for the chosen wavelengths are calculated and then each value is modified by adding a generated noise value (a positive or negative number). When the set of noisy $p(\lambda)$ values is complete giving data for a pseudo-star, values of K , p_{\max} and λ_{\max} are then determined by the normal least squares technique (see Section 2.2).

In order to see how the scatter in K and λ_{\max} behaves, the programme is allowed to free-run 100 times as though a given star with given equipment had been measured independently 100 times. By then changing the p_{\max} , λ_{\max} values over a wide range and repeating the exercise for each set of values, selections from the engendered calculations can be used to mimic any real data set. (The amplitude of the noise function must be set to provide scatter similar to that of the real observations).

3.2 Analysis of Simulated Noisy Data

Firstly, noisy data were generated and analysed for the four colour bands (UBVR) with three values for λ_{\max} occurring in different parts of the above range (0.4, 0.5, 0.6 μ). The behaviour of the derived values of K and λ_{\max} were then investigated when the data were made noisy. The p_{\max} value was set to be equal to 3.0% for all the stars with a standard deviation of a single $p(\lambda)$ measure being approximately 0.04%. The three sets of determined values of K and λ_{\max} are displayed in Fig. 3.1.

It is obvious from the figure that not only are the values of K noisy, as is to be expected, but that there are correlations between the deduced values of K and λ_{\max} , the form being dependent on the true value of λ_{\max} . For a λ_{\max} value in the blue part of the spectrum the deduced values of K and λ_{\max} are related by a positive slope while for λ_{\max} in the red part of the spectrum there is a negative slope.

Scatter in the derived λ_{\max} values for the central λ_{\max} value is much less than for λ_{\max} values either in the blue part or in the red part of the spectrum while the scatter in K is almost the same for the above three values of λ_{\max} .

The overall correlation between K and λ_{\max} for a set of stars will depend on the distributions of the true values of λ_{\max} for the stars and on the magnitude of the noise on the K values, i.e. on the size of the polarimetric noise relative to the p_{\max} value.

More general consideration of the figure would suggest that an overall correlation will ensue if λ_{\max} is given a cut-on or cut-off value. If, for example, the lower limit of λ_{\max} occurs in the blue for which there is a positive slope relating K and λ_{\max} (e.g. see left hand side of Fig. 3.1) then if these data are mixed with other

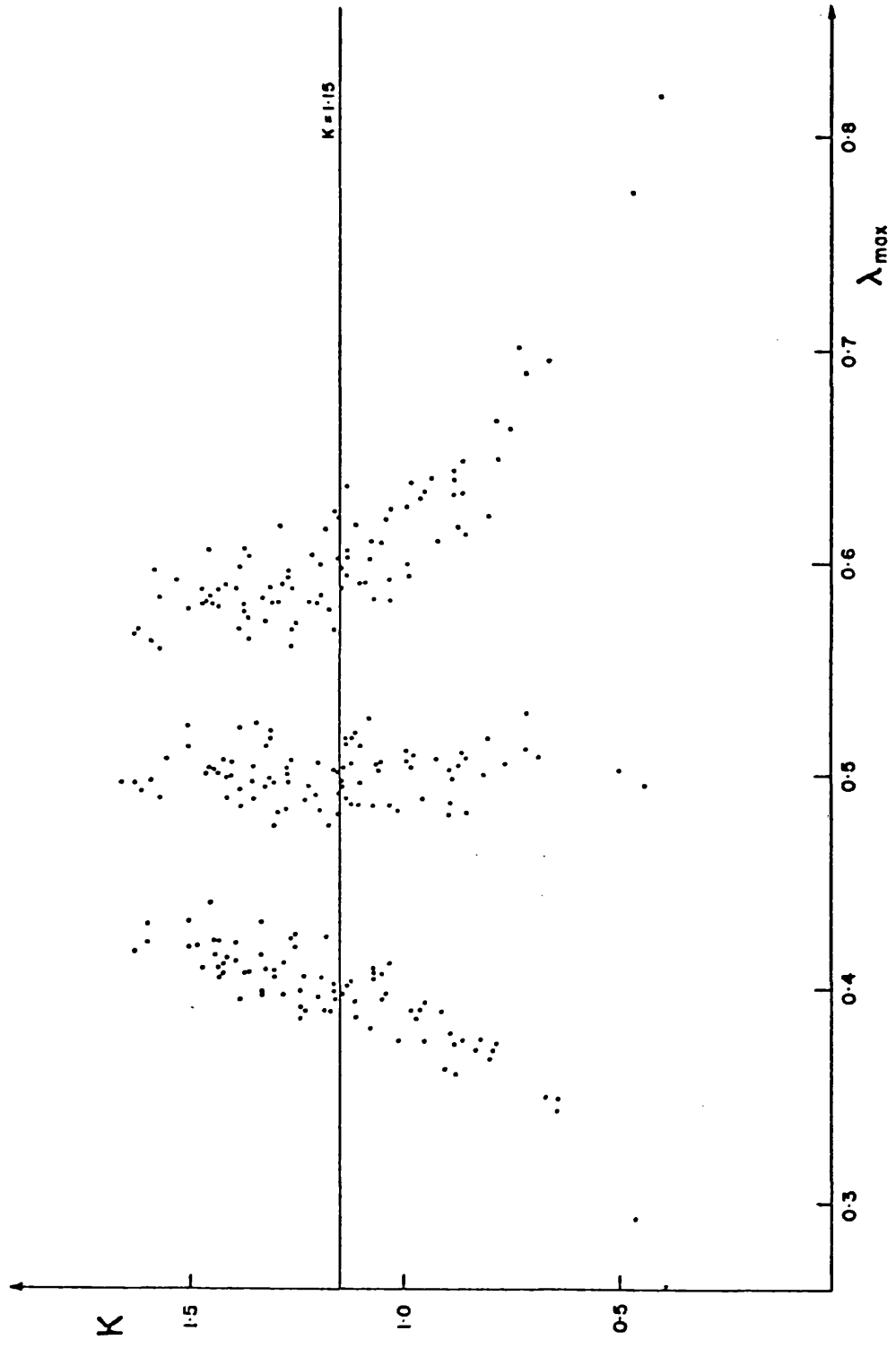


Fig. 3.1 The correlation between K and λ_{\max} for three sets of artificial noisy data with four colours. The plots from left to right are for λ_{\max} values 0.4, 0.5, 0.6 respectively.

data with larger λ_{\max} values, the overall correlation between K and λ_{\max} will tend to be forced at right angles to the positive slope, i.e. the overall correlation will have a negative slope. The problem for this simulation study is one of getting the right mix of stars in terms of their true λ_{\max} values and their relative polarization noises.

As correlations occur between the deduced values of K and λ_{\max} from the artificial noisy data, it was thought that normal experimental noise could be a contributory cause of correlations directly obtained for the real data for both four-colour and seven-colour measurements. Comparisons between the values of K and λ_{\max} from the artificial noisy data with those values from the real data have been made as follows.

The four-colour data have been considered firstly for which the values of K and λ_{\max} are displayed in Fig. 2.1 (SMF data) and Fig. 2.3 (the reduced CGS data). The λ_{\max} values for the artificial data started at 0.45μ and ran to 0.60μ with intervals of 0.025μ , to give values for λ_{\max} covering those values provided by the real observations. The p_{\max} value and the standard deviations were set to be the same as previously selected, i.e. 3.0% and 0.04% respectively.

The programme was run for each value of seven selected λ_{\max} values and the first 25 determined values of K and λ_{\max} for each value have been used for analysis (this selection was assumed to be approximately equivalent to the real data). The 175 values of K and λ_{\max} are displayed in Fig. 3.2. The trend of this simulated data is obvious and the bold solid line represents the least squares best fit with negative slope and is defined by:

$$K = 1.17 - 1.23(\lambda_{\max} - 0.5) \dots\dots\dots 3.1$$

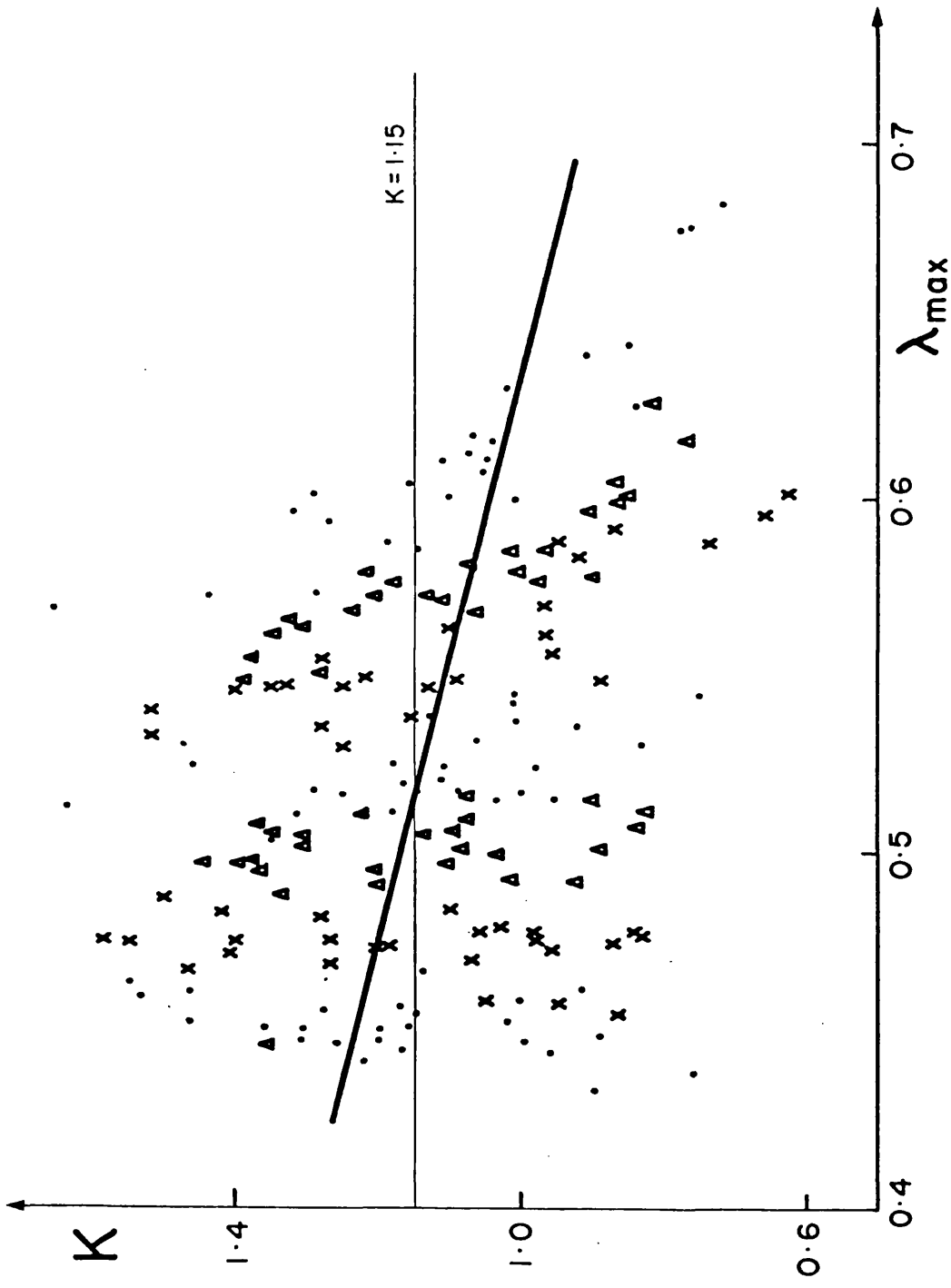


Fig. 3.2 The correlation between K and λ_{\max} for simulated data with four colours corresponding to seven groups of stars with different λ_{\max} values.

From the statistical correlation test (described earlier in Section 2.2) it is found that the above correlation represented by Eq. 3.1 is with 99.9% confidence.

By comparing Eq. 3.1 with the equations relating K and λ_{\max} for the real data, i.e. Eq. 2.5 and Eq. 2.7, we can see the obvious similarity between them.

For the seven-colour data the same values of λ_{\max} have been used and also the same values for p_{\max} and the standard deviations to run the programme. The first ten values of K and λ_{\max} for each set were used for analysis and are displayed in Fig. 3.3. The bold solid line again represents the least squares best fit with positive slope expressed by:

$$K = 1.16 + 0.69(\lambda_{\max} - 0.5) \dots\dots\dots 3.2$$

The above correlation was found to be with 95% confidence. By comparing Eq. 3.2 with Eq. 2.6 which represents the correlation between K and λ_{\max} for the real data (CGS data) we see that both have positive slope but differ in value slightly.

We conclude from the above investigation that the noisy data automatically generate correlations between K and λ_{\max} and that the form of the correlation depends on the position of λ_{\max} relative to the distribution of the effective wavelengths used for measurements as well as on the magnitude of the noise on K . In particular we have seen that for the four-colour simulation (UBVR), the correlation gives a negative slope while for the seven-colour simulation the correlation gives a positive slope, so providing an explanation for the results already obtained from the real data for the two sets, i.e. SMF data and CGS data.

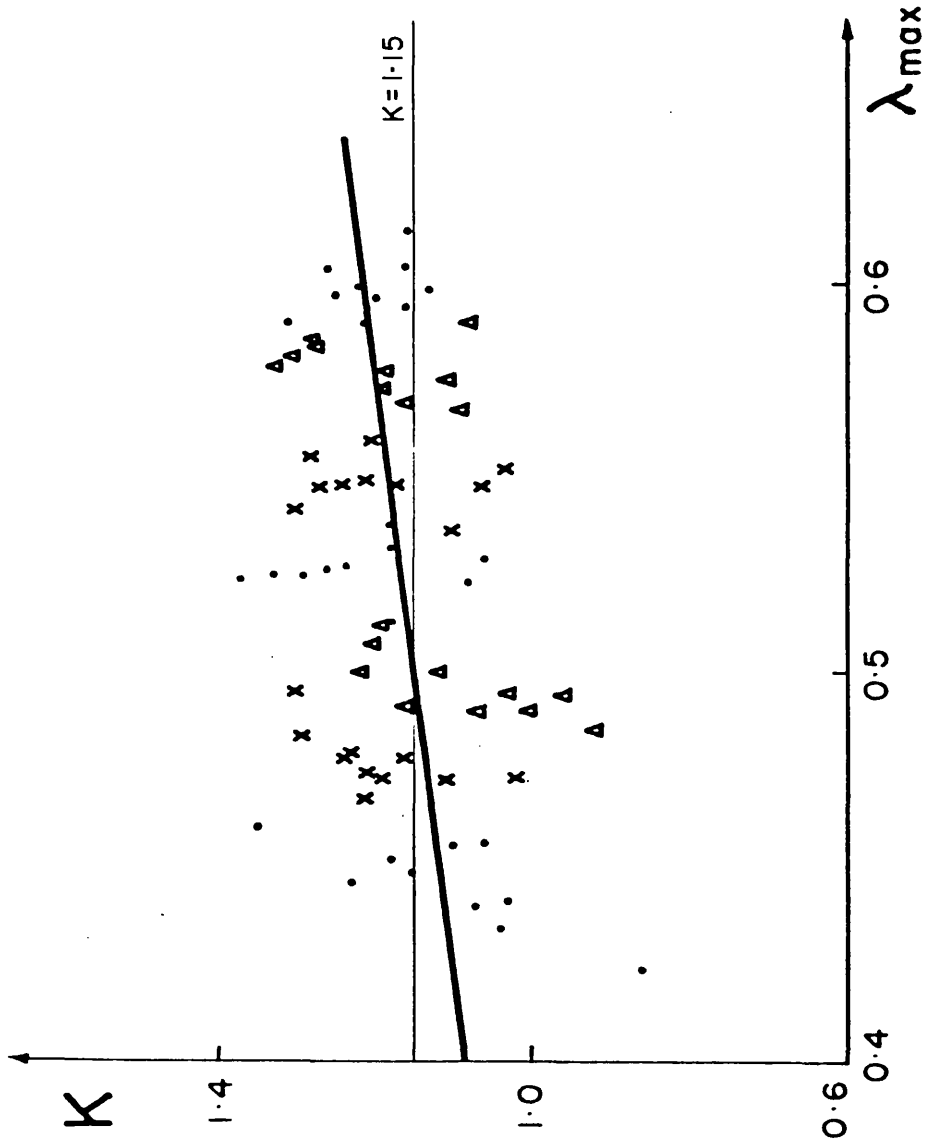


Fig. 3.3 The correlation between K and λ_{\max} for simulated data with seven colours corresponding to seven groups of stars with different λ_{\max} values.

CHAPTER 4

THE ROTATION OF POLARIZATION POSITION ANGLE WITH WAVELENGTH

4.1 Introduction

4.2 The Two-Cloud Model

4.3 The Stars Displaying $\theta(\lambda)$

4.1 Introduction

Following the prediction made by Treanor (1963) that some stars might display dispersion of position angle of interstellar linear polarization, $\theta(\lambda)$, the effect was first observed by Gehrels and Silvester (1965). Confirmation has been provided by Coyne and Gehrels (1966) and later by Serkowski (1968) and Coyne and Wickramasinghe (1969). Observations of $\theta(\lambda)$ are interpreted as being due to the starlight traversing several clouds with different grain alignment and different grain size.

With the discovery of interstellar circular polarization (see Martin, Illing and Angel (1972)) the observations of $\theta(\lambda)$ became more relevant to cloud models as both effects relate to the birefringence of the interstellar medium. The existence of circular polarization in a medium in which the direction of grain alignment changes along the line of sight had been suggested earlier by Serkowski (1962). Hence the birefringence characteristic of the interstellar medium can be derived by combined observations of linear and circular polarization. (Section 4.2).

In addition observations of such a twisted medium could lead to better understanding of the composition of interstellar grains, the mean grain size and any changes in these properties along the line of sight in addition to developing models of the structure within the interstellar medium (Martin (1974)).

The data for 24 stars (in the northern hemisphere) showing significant dispersion of position angle have been collected by Coyne (1974b) (see Table II of that paper). Included in Coyne's list are some stars obviously exhibiting intrinsic polarization for which the $\theta(\lambda)$ can be explained as being due to a superposition of the intrinsic polariza-

tion and interstellar polarization, the wavelength dependence of the combined vector being controlled by the wavelength dependencies of the two components. The late type stars with $\theta(\lambda)$ have not been included in the table as the rotation of position angle may take place primarily in their atmospheres or circumstellar dust shells. A plot of the magnitude and direction of polarization of the 24 stars in galactic co-ordinates has been made. By comparing it with the map of Mathewson and Ford (1970) (see Fig. 1.1) it is found that the $\theta(\lambda)$ effect is quite common near the galactic equator in the range of galactic longitudes $130^\circ - 150^\circ$. Their polarizations tend to follow the overall patterns of the galaxy which in turn means that the mean direction of vibration for these stars is mainly determined by the interstellar medium.

The $\theta(\lambda)$ data have been considered also by Coyne (1974b) in combination with the available data of circular polarization and the proposed model of changing grain alignment and grain size along the line of sight finds support from this analysis. Circular polarization measurements are few and further observations for stars with known $\theta(\lambda)$ would be extremely useful. In addition to Coyne's 24 stars, stars in the southern hemisphere have been observed by SMF showing $\theta(\lambda)$. The curves of $\theta(\lambda)$ are represented in Fig. 4.1, but it must be noted that the figure includes some stars which are intrinsically polarized.

4.2 The Two-Cloud Model

The "Two-Cloud" model has so far been sufficiently satisfactory to interpret the observations of $\theta(\lambda)$ and interstellar circular polarization. (Integral equations are really required to describe the true situations but the complexity of setting them up and solving

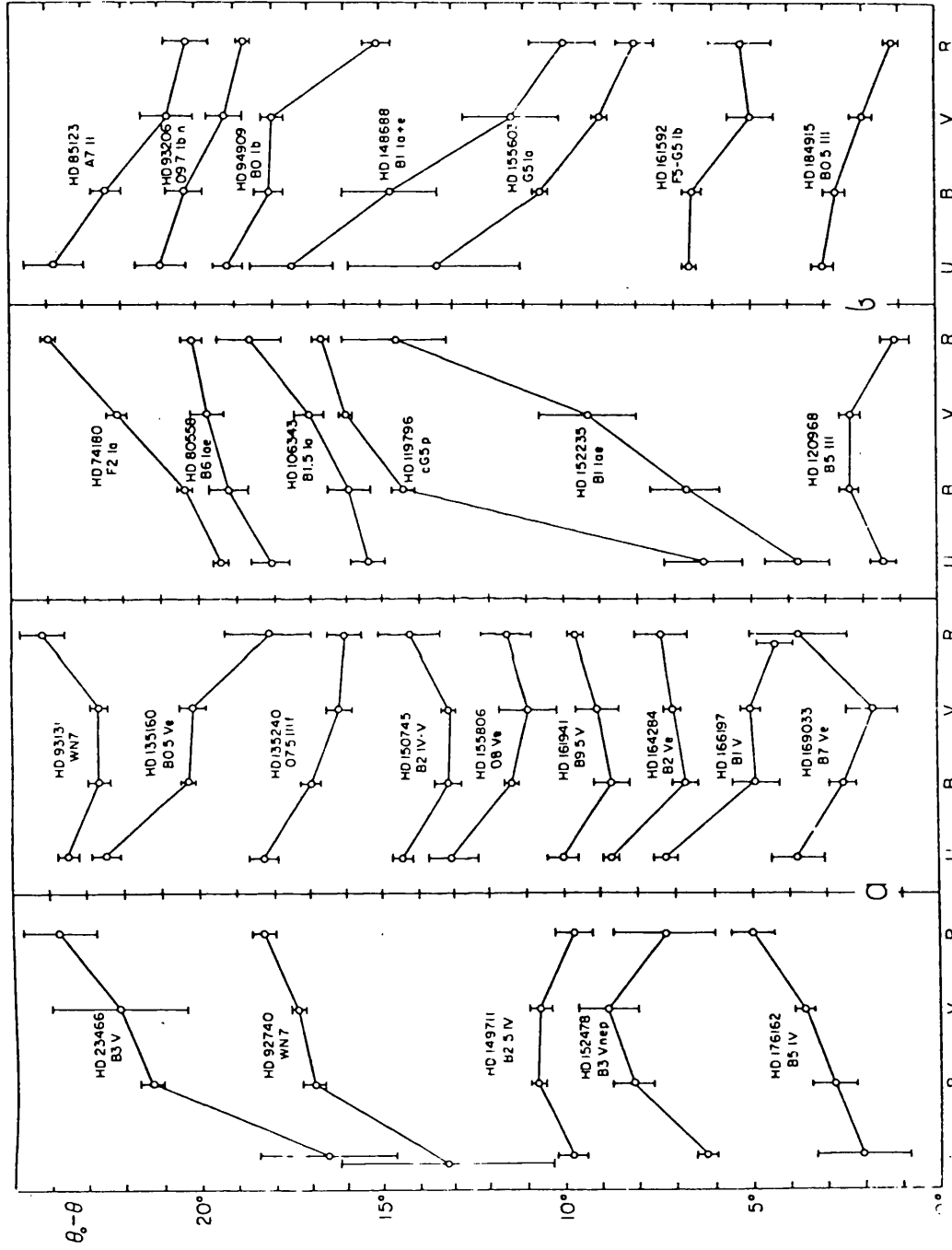


Fig. 4.1 The rotation of polarization position angle with wavelength for stars measured in four colours by SMF (Ref. F4.1)

them has not yet been deemed necessary). Martin (1974, 1978) has developed many models for a medium with changing grain alignment including the two-cloud model which will be discussed more fully here. The following is a résumé of the model.

It is based on the idea that the initial starlight is unpolarized and that two clouds with different dust alignment lie between the star and the observer. It is assumed that the formula of the Serkowski Law can be applied to each cloud in turn. The subscripts 1 and 2 refer to the cloud nearest the star and nearest the observer respectively. The ratio of the linear polarization produced by the clouds may be represented by:

$$r = \frac{p_2}{p_1} \dots\dots\dots 4.1$$

and the difference in their position angles may be denoted by:

$$\phi = \theta_2 - \theta_1 \dots\dots\dots 4.2$$

Because of the misalignment of the two clouds the resultant polarization p_{21} is smaller than the value for $\phi = 0$ by a depolarization factor D expressed by:

$$D^2 = (1 + 2r \cos 2\phi + r^2) / (1 + r^2) \leq 1 \dots\dots\dots 4.3$$

and the circular polarization V/I is:

$$\frac{V}{I} = - \Delta e_2 (p/I)_1 \sin 2\phi \dots\dots\dots 4.4$$

Equation 4.4 shows that the wavelength dependence of circular polarization is the product of the effects of birefringence of the second cloud, Δe_2 , which is acting similarly to a waveplate, converting the linear polarization into circular, and the dichroism of the

first cloud, $(p/I)_1$. If Cloud 2 is uniform then the factor describing the geometry of the alignment in the interstellar medium is:

$$G = -r \sin 2\phi / (1 + 2r \cos 2\phi + r^2) \dots\dots\dots 4.5$$

G and r will be wavelength dependent when wavelength dependencies of linear polarization produced by the two clouds differ.

The observed position angle, θ_1 , is given by:

$$\tan 2(\theta - \theta_1) = r \sin 2\phi / (1 + r \cos 2\phi) \dots\dots\dots 4.6$$

This in turn will be wavelength dependent if r is provided that $\phi \neq 0$.

By differentiating θ with respect to wavelength λ we obtain:

$$\frac{d\theta}{d\lambda} = 0.5 G d \ln r / d\lambda \dots\dots\dots 4.7$$

or
$$\frac{d\theta}{d\lambda} = 0.5 \frac{dr}{d\lambda} (\sin 2\phi) / (1 + r^2 + 2r \cos 2\phi) .$$

If r is evaluated in Eq. 4.7 on the basis of the Serkowski Law (Eq. 1.1) a valuable formula for the change of grain size along the line of sight ensues as follows:

$$\frac{\lambda_{\max 2}}{\lambda_{\max 1}} = \exp \left(- \frac{1}{1.15} \frac{\lambda}{G} \frac{d\theta}{d\lambda} \right) \dots\dots\dots 4.8$$

or
$$\frac{d\theta}{d\lambda} = - \frac{Kr (\sin 2\phi)}{\lambda(1 + 2r \cos 2\phi + r^2)} \ln \frac{\lambda_{\max 2}}{\lambda_{\max 1}} .$$

From this equation expressing $\frac{d\theta}{d\lambda}$, we see that θ has a maximum when $\lambda = \infty$, $\phi = 0$, $r = 0$, or when $\lambda_{\max 1} = \lambda_{\max 2}$, otherwise the change of position angle with wavelength will simply be monotonic. (The results of our numerical calculations confirm this).

The above model has been applied to two stars σ Sco and \omicron Sco for which both linear and circular polarization data are available

and the resulting analysis was sufficiently consistent (see Martin (1974)).

McMillan and Tapia (1977) in their survey to investigate $p(\lambda)$ in the Cyg OB2 association have shown that the polarization can be satisfactorily represented by the two-cloud model and claim to have determined the interstellar birefringence of the medium in front of Cyg OB2 No. 12. The first cloud which is nearest the star is characterised by $P_{\max_1} = 11.3\%$, $\lambda_{\max_1} = 0.49$, $\theta_1 = 125^\circ$, while the second cloud is characterised by $P_{\max_2} = 3.4\%$, $\lambda_{\max_2} = 0.52$, $\theta_2 = 57^\circ$. By letting f_1 and f_2 refer to λ_{\max_1}/λ and λ_{\max_2}/λ respectively, Equation 25 in Martin's (1974) paper has been used to determine the interstellar birefringence which is then expressed by the authors as:

$$b(f_2) = \frac{-q(f_2)}{P_{\max_2} P_{\max_1} d(f_1) \sin 2\phi} \dots\dots\dots 4.9$$

where $q(f_2)$ is the observed circular polarization and $d(f_1)$ is the standard wavelength dependence of linear polarization in the first cloud. The circular polarization measurements at three wavelengths for the star No. 12 by Martin and Angel (1976) have been used to calculate the values of $b(f_2)$. The ratio λ_{\max}/λ_c was found to be 1.02 ± 0.05 for the medium in front of this star which is closer to the average interstellar mean value than Martin and Angel's value. The G parameter was calculated as well and an excellent agreement was obtained with those values of Martin and Angel, although the latter authors used a different method. Table 6 of that paper summarises all the results.

In the following section the available data for stars displaying $\theta(\lambda)$ will be analysed with respect to Serkowski's Law.

4.3 The Stars Displaying $\theta(\lambda)$

The single cloud of aligned interstellar grains has been considered largely to interpret the observed polarization for the hundreds of stars for which the position angle does not vary with wavelength. All the measurements of $p(\lambda)$ for these stars give a maximum value of polarization, p_{\max} , at some wavelength λ_{\max} , within the visible to near infrared of the spectrum; the empirical formula of Serkowski's Law generally gives a satisfactory match for the normalised curve of the observations of $p(\lambda)$.

For the stars which display $\theta(\lambda)$ (with no apparent intrinsic polarization) the model of two clouds with different grain size, different λ_{\max} , and grain alignment, as we have seen in Sections 4.1, 4.2, is accepted as being sufficient for an interpretation. The combined effect of two such clouds will undoubtedly affect the value of K , this being a measure of the sharpness or halfwidth of the $p(\lambda)$ curve. With this in mind it was thought worthwhile to compare the values of K for stars which show $\theta(\lambda)$ and for those without rotation of position angle. The data available for the stars displaying $\theta(\lambda)$ are contained in two papers, Coyne (1974b) and SMF. The same procedure of the least squares solution which was described earlier (see Section 2.2) has been used to refit the data for these stars to the general Serkowski Law, with K as a free parameter (the same range $0.2 \rightarrow 1.7$ was allowed for K).

The procedure was first applied to Coyne's data (mainly with seven colours) with the number of stars for analysis being 19. From these it was found that the line relating K and λ_{\max} has negative slope with the least squares fit being expressed by:

$$K = 1.02 - 1.27(\lambda_{\max} - 0.5) \dots\dots\dots 4.10$$

We see that the relation between K and λ_{\max} for the above stars shows an opposite slope in comparison with the stars in the single cloud situation when measured over the same range of wavelength (see Fig. 2.2).

The SMF data are depicted in Fig. 10 of that paper (see Fig. 4.1 here) with the stars designated by their HD number. Included in the figure are some intrinsically polarized stars. These latter stars are excluded from the analysis here. The number of stars provided for analysis from SMF is 16. These stars have been combined with those from Coyne for which the measurements have been reduced to four colours closest to UBV bands. The total number of stars measured in four colours and displaying $\theta(\lambda)$ is now 31. The slope relating K and λ_{\max} for these stars is negative with the best straight line of the least squares being expressed by:

$$K = 1.11 - 1.52(\lambda_{\max} - 0.5) \dots\dots\dots 4.11$$

Comparisons between Equations 4.10 and 4.11 with the relationships of K and λ_{\max} for stars not displaying $\theta(\lambda)$, have been made as follows:

For SMF data the 107 stars for which the K and λ_{\max} values are available have been divided into seven different groups, each group consisting of 31 stars, being equal to the number of stars which display $\theta(\lambda)$, and the least squares straight line fit was obtained for each group. Fig. 4.2 represents these seven lines (solid lines) while Equation 4.11 is depicted as the broken line. It is obvious that the latter line is displaced from the others showing that these stars generally provide lower values of K (less than 1.15). In a similar way, a comparison has been made for the stars with seven-colour measurements. Here the 73 stars have been divided into four groups, each one comprising 19 stars which corresponds to the number of stars with

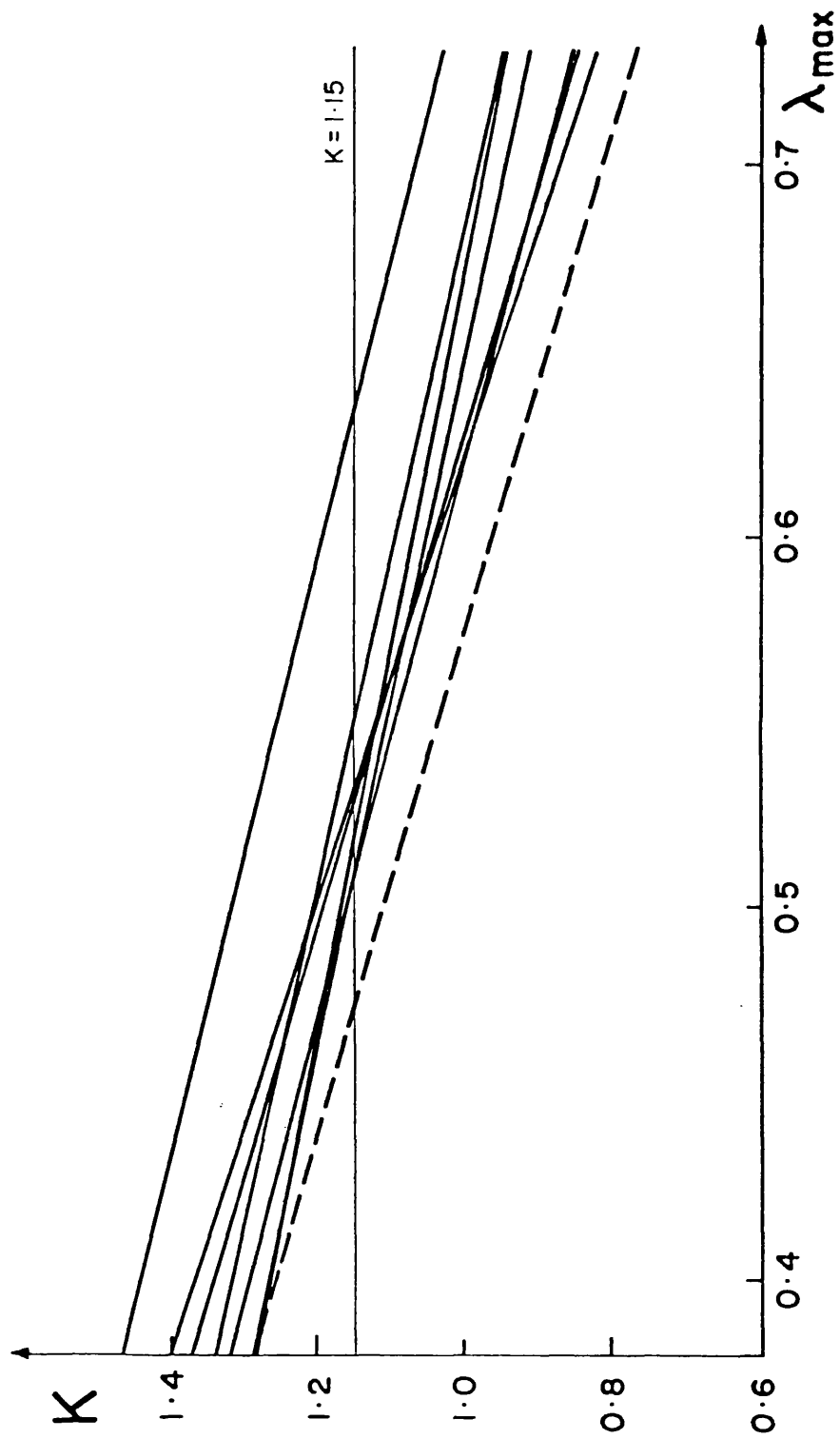


Fig. 4.2 The comparison between the best line relating K and λ_{\max} for stars showing $\theta(\lambda)$ (broken line) with the lines for different groups of stars without rotation of polarization angle (solid lines). These data are for four-colour measurements.

$\theta(\lambda)$ measured over the same range of wavelengths. Fig. 4.3 represents the least squares straight line fit (solid lines) for the four groups of stars while the dotted line represents the fit (Equation 4.10) for the stars with $\theta(\lambda)$. We see again how this last line is significantly different from stars not displaying $\theta(\lambda)$. Low values of K occur for the whole range of λ_{\max} compared with the normal stars; the slope also has the opposite sense.

The change in slope for the seven-colour data for stars showing $\theta(\lambda)$ is difficult to explain on the basis of any cloud model. However when the stars are re-examined individually, it is evident that some of them carry intrinsic polarization and therefore should not be included in the overall correlation study. In particular two stars have extreme values of λ_{\max} with low K value and obviously contribute strongly to the negative slope. Inspection of Table II of Coyne (1974) suggests that these stars (HD 10516 and HD 37061) do in fact exhibit intrinsic polarization by virtue of θ being time dependent, $\theta(t)$, and should therefore be removed from the study. With the exclusion of these two stars a reassessment of the correlation between K and λ_{\max} now reverts to show a positive slope expressed by:

$$K = 1.02 + 0.96(\lambda_{\max} - 0.5) \dots\dots\dots 4.12$$

The above relationship is represented in Fig. 4.3 as a long-dashed line and is obviously showing the displacement from the other lines for data without rotation of polarization position angle, giving the low values of K .

Three other stars (HD 192422, HD 141637, HD 159176) in Coyne's table are also designated as displaying $\theta(t)$ and should also be ignored. Another star (HD 169454) is listed as showing possible $\theta(t)$ but it can be noted that it does not provide a value of K in the

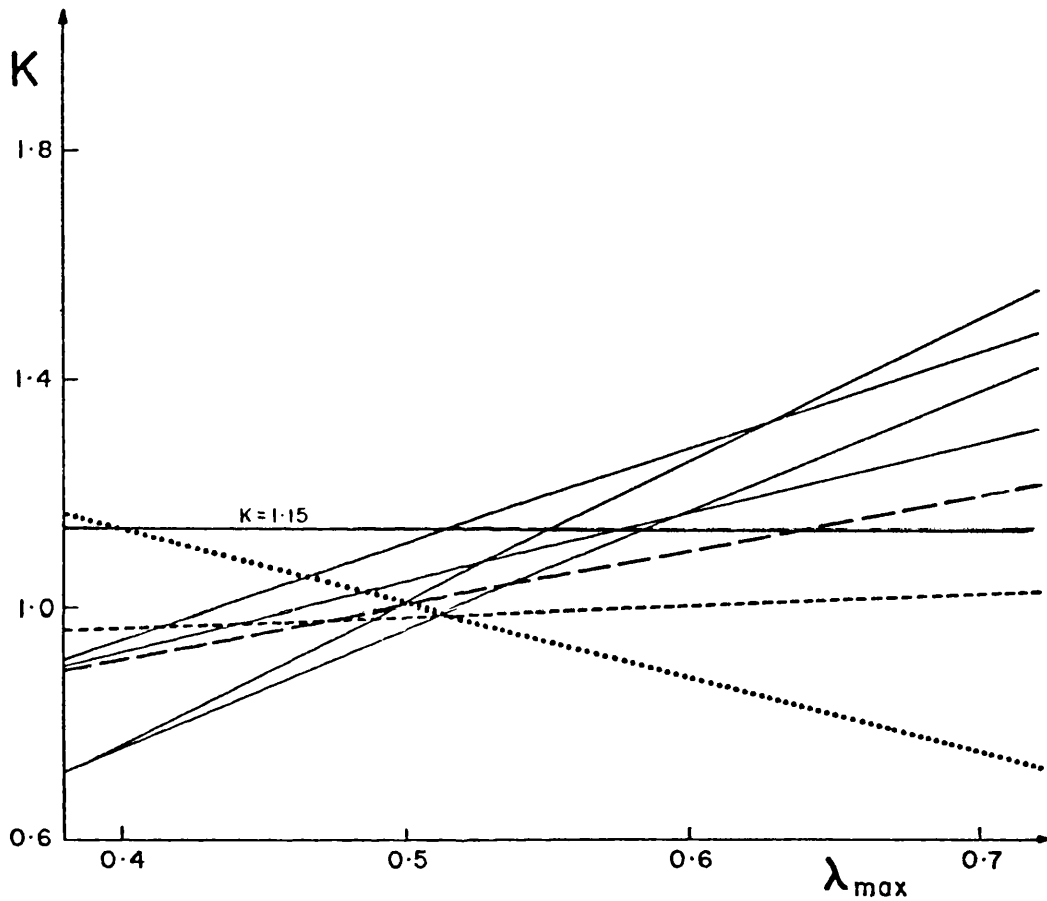


Fig. 4.3 The comparison between the best line relating K and λ_{\max} for stars showing $\theta(\lambda)$ (dotted line) and the lines after excluding the stars showing $\theta(t)$ (long-dashed line and short-dashed line) with the lines for different groups of stars without rotation of polarization position angle (solid lines). These data are for seven-colour measurements.

permitted range and has already been excluded automatically. With the exclusion of all the stars showing $\theta(t)$ the relation between K and λ_{\max} for the remaining stars again has positive slope expressed by:

$$K = 0.98 + 0.13(\lambda_{\max} - 0.5) \quad \dots\dots\dots 4.13$$

The above equation is represented as a short-dashed line in Fig. 4.3 which is based now on only 14 stars and it cannot be expected to have a high confidence level. Even now, some of these stars may carry weak levels of intrinsic polarization but it is assumed that this is not affecting the general conclusion.

Thus the overall picture appears to be coherent. For both the four-colour and seven-colour data, stars which exhibit $\theta(\lambda)$ provide a K, λ_{\max} correlation similar to stars not displaying the dispersion, except that the level of K is reduced.

A simple interpretation for K taking values different from 1.15 has already been mentioned in terms of the Two-Cloud model. In the following chapter we shall investigate the properties of K numerically for this model. This aspect has been neglected in the literature for the development of the model and the new results provide means for discussion of the reasons behind the different correlations presented in Figs. 4.2 and 4.3.

CHAPTER 5

A NUMERICAL INVESTIGATION OF THE TWO-CLOUD MODEL

5.1 Introduction

5.2 The Two-Cloud Model

5.1 Introduction

The programme described below aimed to calculate the polarization produced by two clouds with different λ_{\max} and different orientation which has been sufficient so far to model a complex cloud situation. The data for the resultant polarization were afterwards fitted to the general formula of Serkowski's Law to see the behaviour of the deduced characteristic parameters, λ_{\max} and K, over all possible orientations of the clouds and for a range of cloud characteristics (i.e. λ_{\max_1} , λ_{\max_2} , P_{\max_1} , P_{\max_2}). The following is a description of the model.

5.2 The Two-Cloud Model

The model is based on the same idea as developed by Martin (1974, 1978) and the same notation for the subscripts has been used, i.e. subscripts 1 and 2 refer to the cloud nearest the star and nearest the observer respectively. It is also assumed that the initial starlight is unpolarized.

The Stokes parameters and Mueller calculus is found to be an adequate way to describe the polarization state of the light and its behaviour as it passes through media, and has been used by many workers in the field of astronomical polarimetry.

Let the Stokes parameters be denoted by I, Q, U, V where:

I represents the intensity

Q, U represent the components of the linear polarization

V represents the component of the circular polarization.

(N.B. Other letters are used for labelling the parameters by different workers (see Table 1.2 of Clarke and Grainger (1971) for more details).

These parameters can be grouped together to form a vector known

as the Stokes vector which represents the complete polarization characteristics of the light. For the initial light which is unpolarized the Stokes vector is represented by:

$$\begin{bmatrix} I \\ Q \\ U \\ V \end{bmatrix} = \begin{bmatrix} I \\ 0 \\ 0 \\ 0 \end{bmatrix} = I \begin{bmatrix} 1 \\ 0 \\ 0 \\ 0 \end{bmatrix}$$

After traversing the first cloud the normalised vector will be:

$$\begin{bmatrix} I \\ Q \\ U \\ V \end{bmatrix} = (I - A_1) \begin{bmatrix} 1 \\ p_1 \cos 2\theta_1 \\ p_1 \sin 2\theta_1 \\ 0 \end{bmatrix}$$

and after traversing the second cloud the normalised vector will be:

$$\begin{bmatrix} I \\ Q \\ U \\ V \end{bmatrix} = (I - A_1 - A_2) \begin{bmatrix} 1 \\ p_1 \cos 2\theta_1 + p_2 \cos 2\theta_2 \\ p_1 \sin 2\theta_1 + p_2 \sin 2\theta_2 \\ 0 \end{bmatrix}$$

where A_1 and A_2 are the absorptions produced by the first and second cloud respectively. For simplicity it has been assumed that the polarized intensity produced by the first cloud is not acted upon by the second. If the orientation of the first cloud is taken as reference for the system, i.e. $\theta_1 = 0$, and by letting $\theta_2 = \phi$ the algebra is simplified and the normalised Stokes vector reduces to:

$$\begin{bmatrix} I \\ Q \\ U \\ V \end{bmatrix} = (I - A_1 - A_2) \begin{bmatrix} 1 \\ p_1 + p_2 \cos 2\phi \\ p_2 \sin 2\phi \\ 0 \end{bmatrix}$$

The resultant degree of polarization produced by the effect of the two clouds will be:

$$\begin{aligned}
 p &= (Q^2 + U^2)^{\frac{1}{2}} \\
 p^2 &= (p_1 + p_2 \cos 2\phi)^2 + (p_2 \sin 2\phi)^2 \\
 p &= (p_1^2 + p_2^2 + 2p_1p_2 \cos 2\phi)^{\frac{1}{2}} \quad \dots\dots\dots 5.1
 \end{aligned}$$

The position angle, ζ , is given by:

$$\tan 2\zeta = \frac{U}{Q} = \frac{p_2 \sin 2\phi}{p_1 + p_2 \cos 2\phi}$$

Hence
$$\zeta = \frac{1}{2} \tan^{-1} \left(\frac{p_2 \sin 2\phi}{p_1 + p_2 \cos 2\phi} \right) \quad \dots\dots\dots 5.2$$

If the two clouds have identical alignment Equation 5.1 reduces to:

$$p = p_1 + p_2$$

i.e. the polarization produced by the two clouds equals the sum of the polarizations produced by each cloud. In addition, ζ will go to zero. Therefore we do not expect ζ to display dispersion unless $\phi \neq 0$.

The formula of Serkowski's Law has been applied to determine the polarization of each cloud at wavelength points within $0.33\mu \rightarrow 0.95\mu$. Seven colours were chosen in this range to match Coyne's 7-colour data.

The programme allows the choice of λ_{\max} and p_{\max} values for each cloud in addition to their relative orientation for evaluation of Equations 5.1 and 5.2. The λ_{\max} and p_{\max} values used for this exercise provided ratios of $\lambda_{\max_1}/\lambda_{\max_2} = R_\lambda = 0.5, 0.57, 0.67, 0.8$ and $p_{\max_1}/p_{\max_2} = R_p = 1, 0.5, 0.33, 2, 3$. The relative orientation values (ϕ) cover the range $0^\circ \rightarrow 90^\circ$.

The calculations of the resultant polarization and the corresponding position angle in the above wavelength range have been repeated for each value of ϕ commencing at $\phi = 0$ with increments of 5° . For each

value of the ratio R_λ the five values of the ratio R_p have been used in the calculations. The evaluated data of $\zeta(\lambda)$ for the whole range of λ_{\max} , p_{\max} and ϕ confirmed that the change of the position angle with wavelength is monotonic (see Section 4.2, Eq. 4.8).

The same procedure of the least squares solution which has been applied previously to the other spectropolarimetric data (see Section 2.2), has been used here to fit the polarization data produced by the Two-Cloud model.

Plots of K and λ_{\max} values as a function of ϕ have been made for each value of R_λ and for the different values of R_p . Figures 5.1, 5.2, 5.3, 5.4 represent the plots of K against ϕ for R_λ values 0.5, 0.57, 0.67, 0.8 respectively. We see from the figures that the combined effect of the two clouds dramatically affects the values of K for all the values of λ_{\max} and p_{\max} of the two clouds.

It can be seen from the figures that the values of K are generally reduced relative to $K = 1.15$ for the orientation values ranging approximately from $0 \rightarrow 70^\circ$, otherwise K takes values larger than 1.15 unless $R_p = 1$. In addition, for this same ratio, we can see the common effect from all the figures that K takes the lowest values compared with the values for the other R_p values. On the other hand, the K values become closer to 1.15 as R_λ goes to unity. We conclude that the K values show dependencies on the clouds' characteristic parameters, i.e. R_λ , R_p and their relative orientation.

Plots of λ_{\max} against ϕ are represented in Figures 5.5, 5.6, 5.7 and 5.8 for the values of R_λ 0.5, 0.57, 0.67, 0.8 respectively. From inspection of the figures, we can see the similarity in the behaviour of the curves for the above values of R_λ .

The chief features can be summarised as follows.

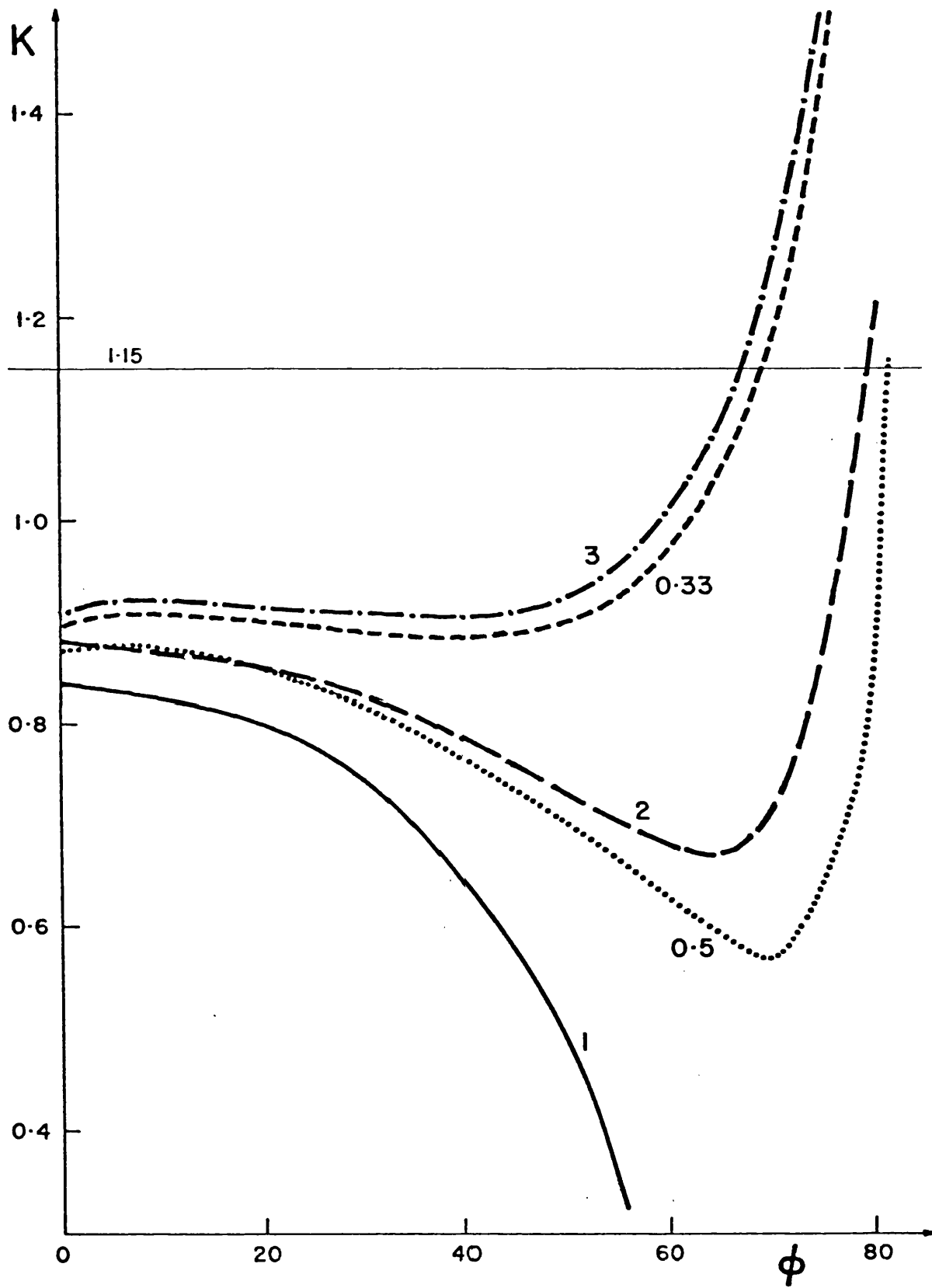


Fig. 5.1 Plots of K values against the relative orientation (ϕ) of the two clouds for $R_\lambda = 0.5$ and for $R_p = 1, 0.5, 0.33, 2, 3$, as marked on the curves.

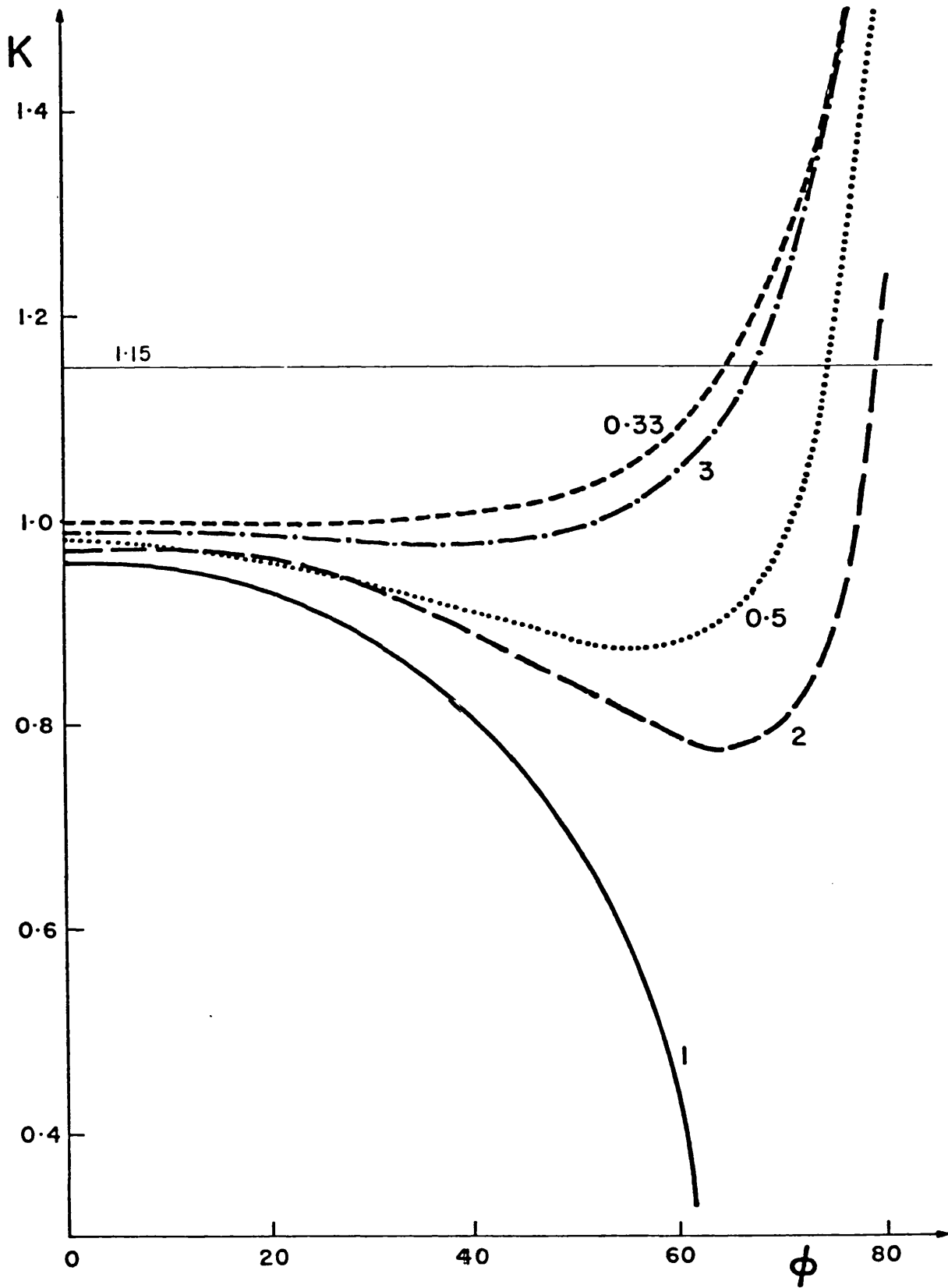


Fig. 5.2 Plots of K values against the relative orientation (ϕ) of the two clouds for $R_\lambda = 0.57$ and for $R_p = 1, 0.5, 0.33, 2, 3$, as marked on the curves.

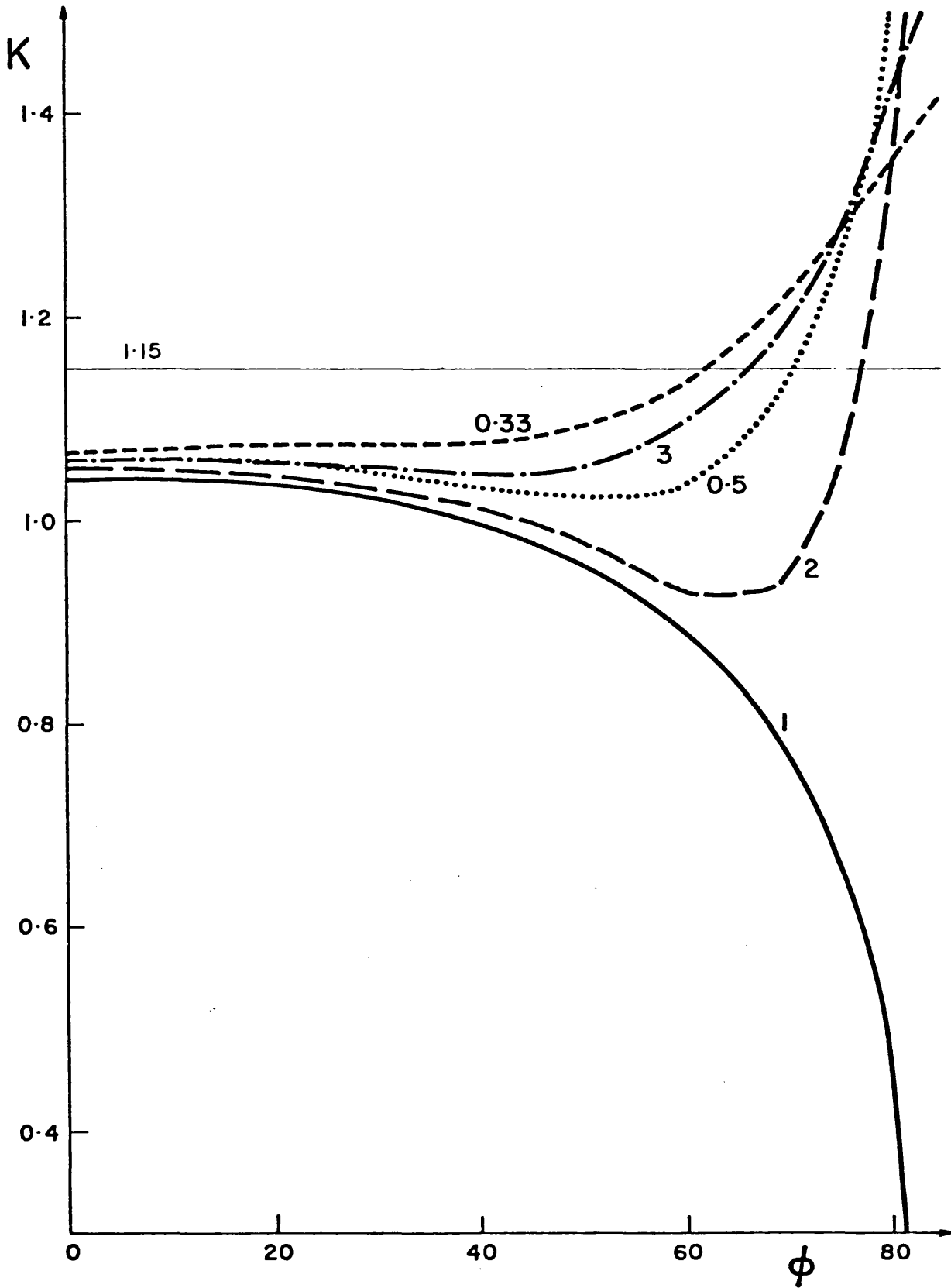


Fig. 5.3 Plots of K values against the relative orientation (ϕ) of the two clouds for $R_\lambda = 0.67$ and for $R_p = 1, 0.5, 0.33, 2, 3$, as marked on the curves.

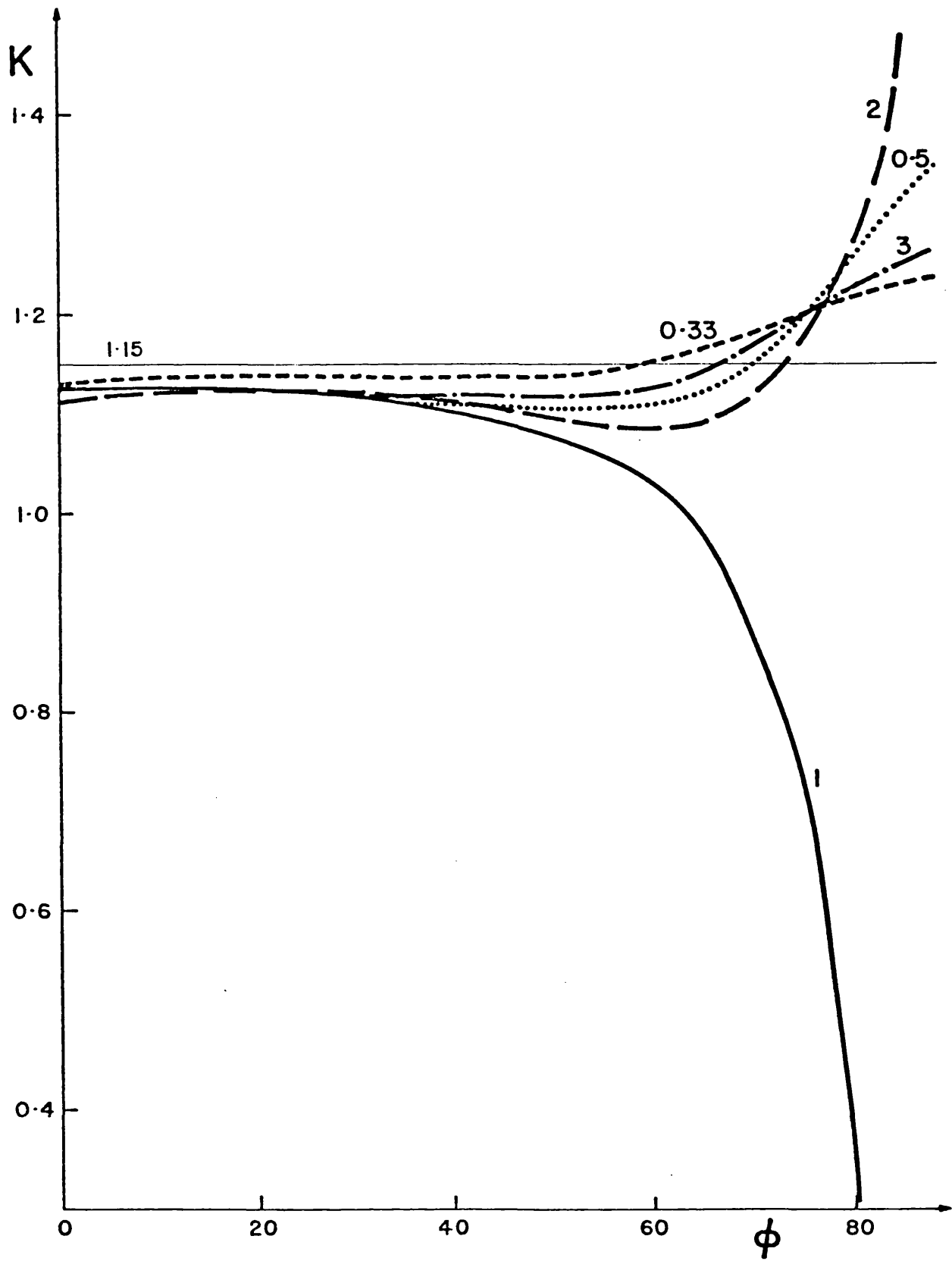


Fig. 5.4 Plots of K values against the relative orientation (ϕ) of the two clouds for $R_\lambda = 0.8$ and for $R_p = 1, 0.5, 0.33, 2, 3$, as marked on the curves.

1. When the two clouds are of the same strength, i.e. $P_{\max_1} = P_{\max_2}$, the derived λ_{\max} values are constant with ϕ for the whole range of R_λ . For any particular R_λ ratio, the derived constant value of λ_{\max} for $P_{\max_1} = P_{\max_2}$ lies within the range of values provided by other ratio values given when $R_p \neq 1$. In addition this value is always lower than the mean of the original values of λ_{\max} for the two clouds, i.e.

$$\lambda_{\max} < \left(\frac{\lambda_{\max_1} + \lambda_{\max_2}}{2} \right) .$$

2. The derived λ_{\max} values are larger than the mean when the strength of the foreground cloud is greater than that of the cloud nearest the star, i.e. $P_{\max_2} > P_{\max_1}$. These values are increased with increasing ϕ for all the values of R_λ . On the other hand, the smaller values of λ_{\max} occur when the strength of the foreground cloud is less than that of the cloud nearest the star, i.e. $P_{\max_2} < P_{\max_1}$, and are decreased with increasing ϕ again for the whole range of R_λ . We see that these characteristics of the λ_{\max} behaviour depend on the parameters describing the two clouds.

In summary, we can see that both the deduced K and λ_{\max} are affected by the two-cloud situation and that, in general, for small values of ϕ , the K value is reduced and the λ_{\max} value always lies between the original λ_{\max} values for the separate clouds.

The position angles of the resultant polarization have been analysed according to ϕ . Here we aimed to investigate which filters are perhaps the most appropriate for detecting $\theta(\lambda)$ variations at the telescope according to the value of ϕ .

Firstly we chose two different pairs, the first one corresponding to the filters 0.943μ and 0.429μ , ($\theta_I - \theta_B$), and the second corresponding to the filters 0.826μ and 0.36μ , ($\theta_R - \theta_U$). These have been investigated with respect to ϕ for the value of R_λ equal to 0.5.

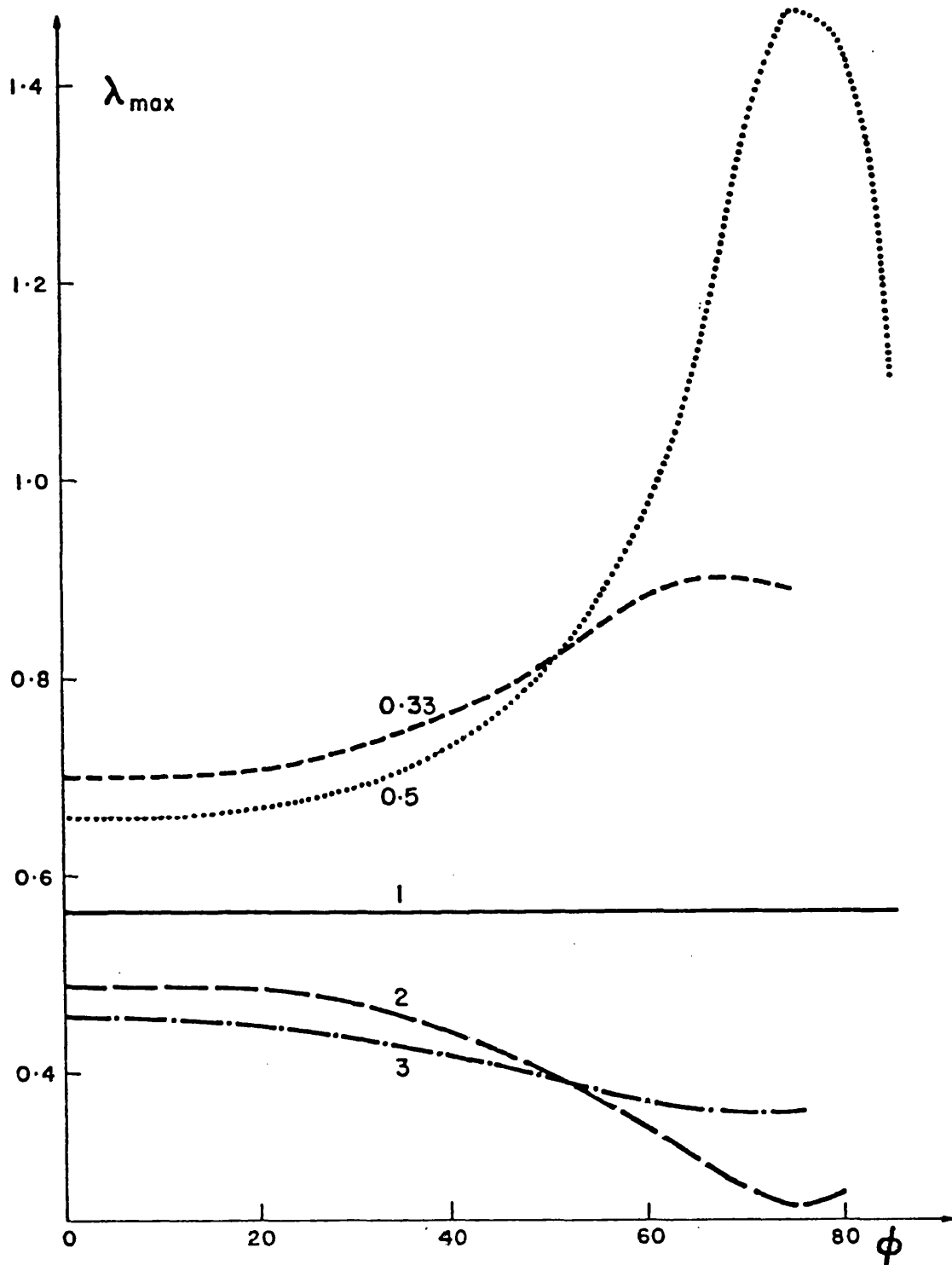


Fig. 5.5 Plots of λ_{\max} values against the relative orientation (ϕ) of the two clouds for $R_{\lambda} = 0.5$ and for $R_p = 1, 0.5, 0.33, 2, 3$, as marked on the curves.

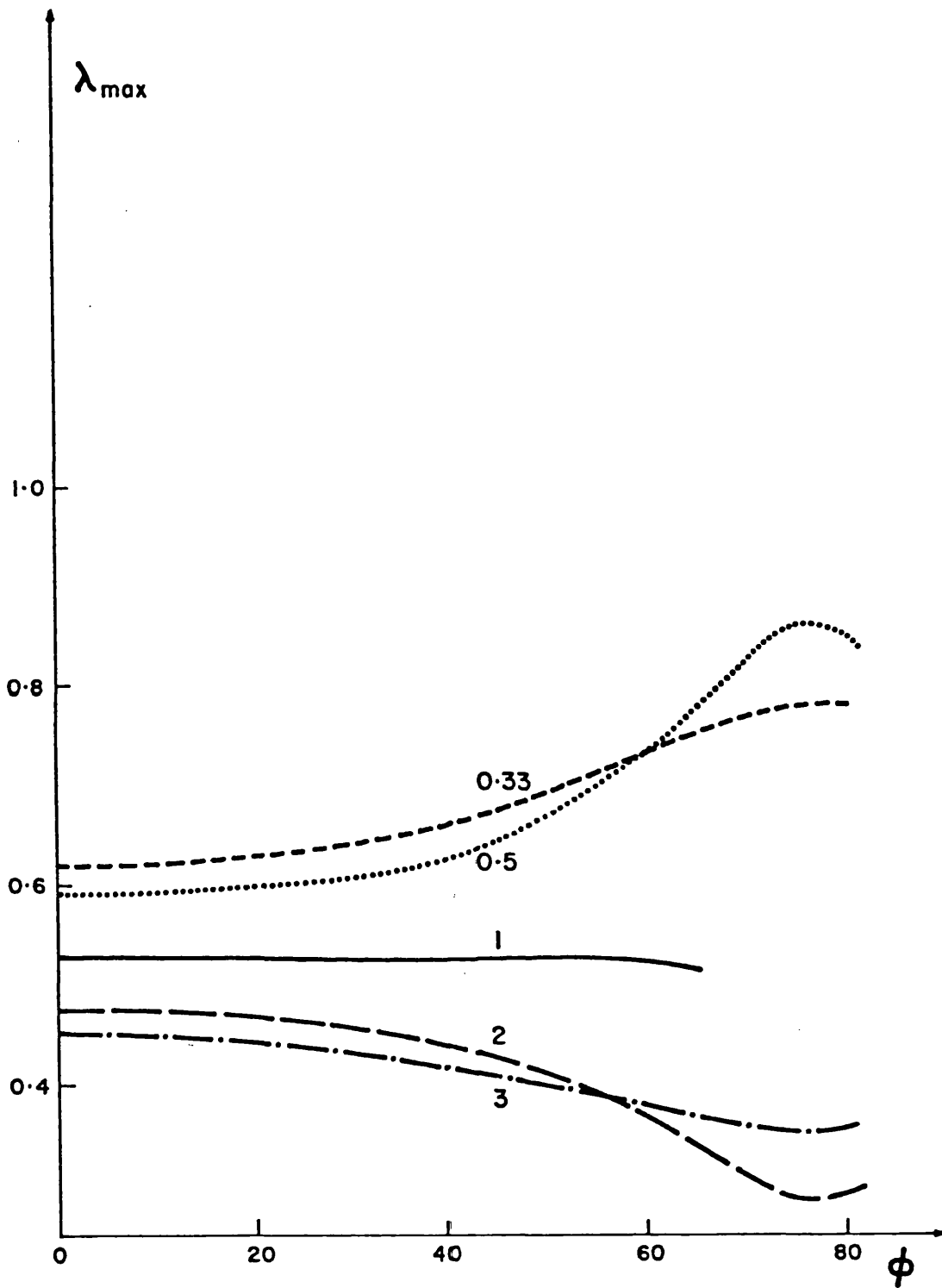


Fig. 5.6 Plots of λ_{\max} values against the relative orientation (ϕ) of the two clouds for $R_\lambda = 0.57$ and for $R_p = 1, 0.5, 0.33, 2, 3$, as marked on the curves.

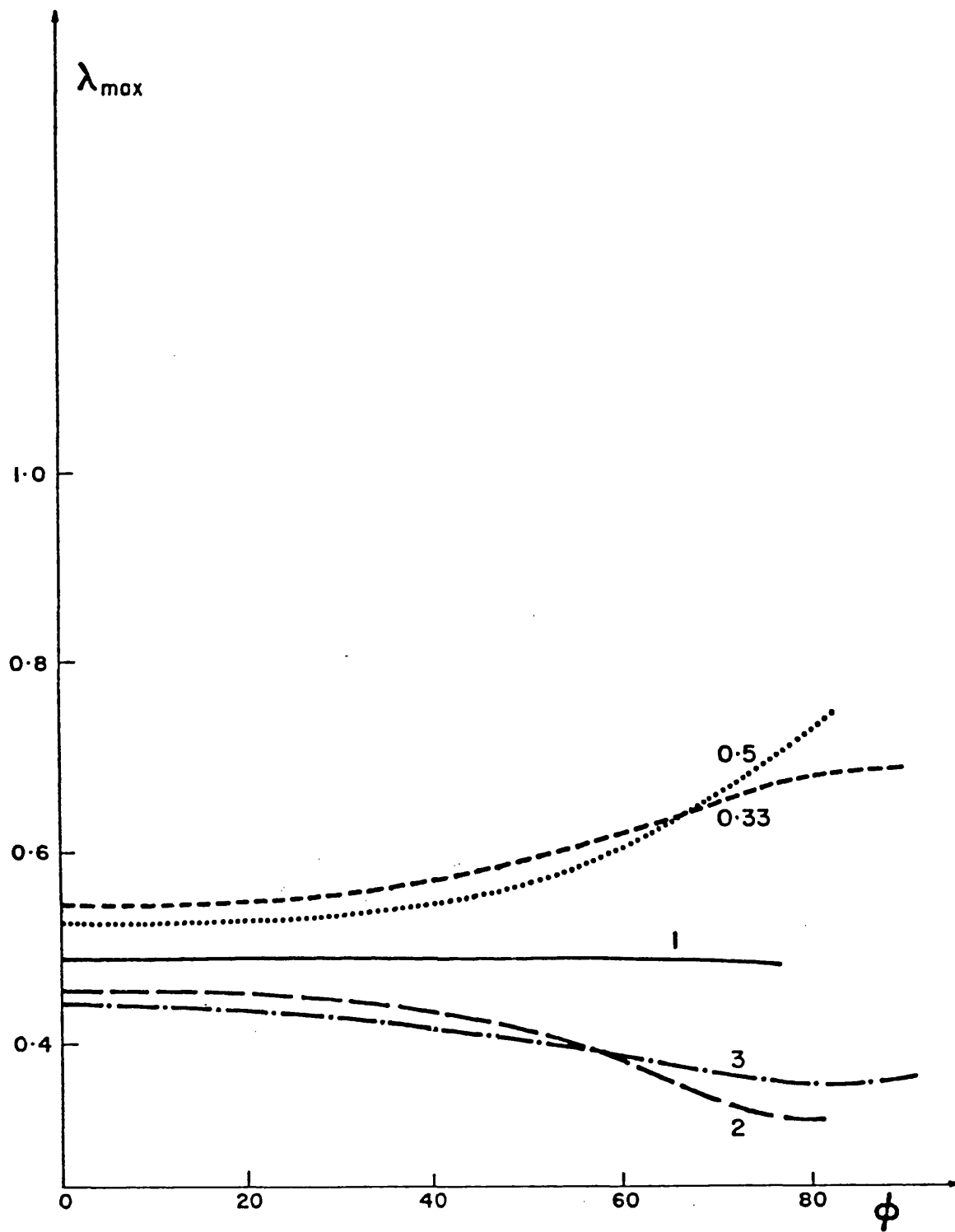


Fig. 5.7 Plots of λ_{\max} values against the relative orientation (ϕ) of the two clouds for $R_{\lambda} = 0.67$ and for $R_p = 1, 0.5, 0.33, 2, 3$, as marked on the curves.

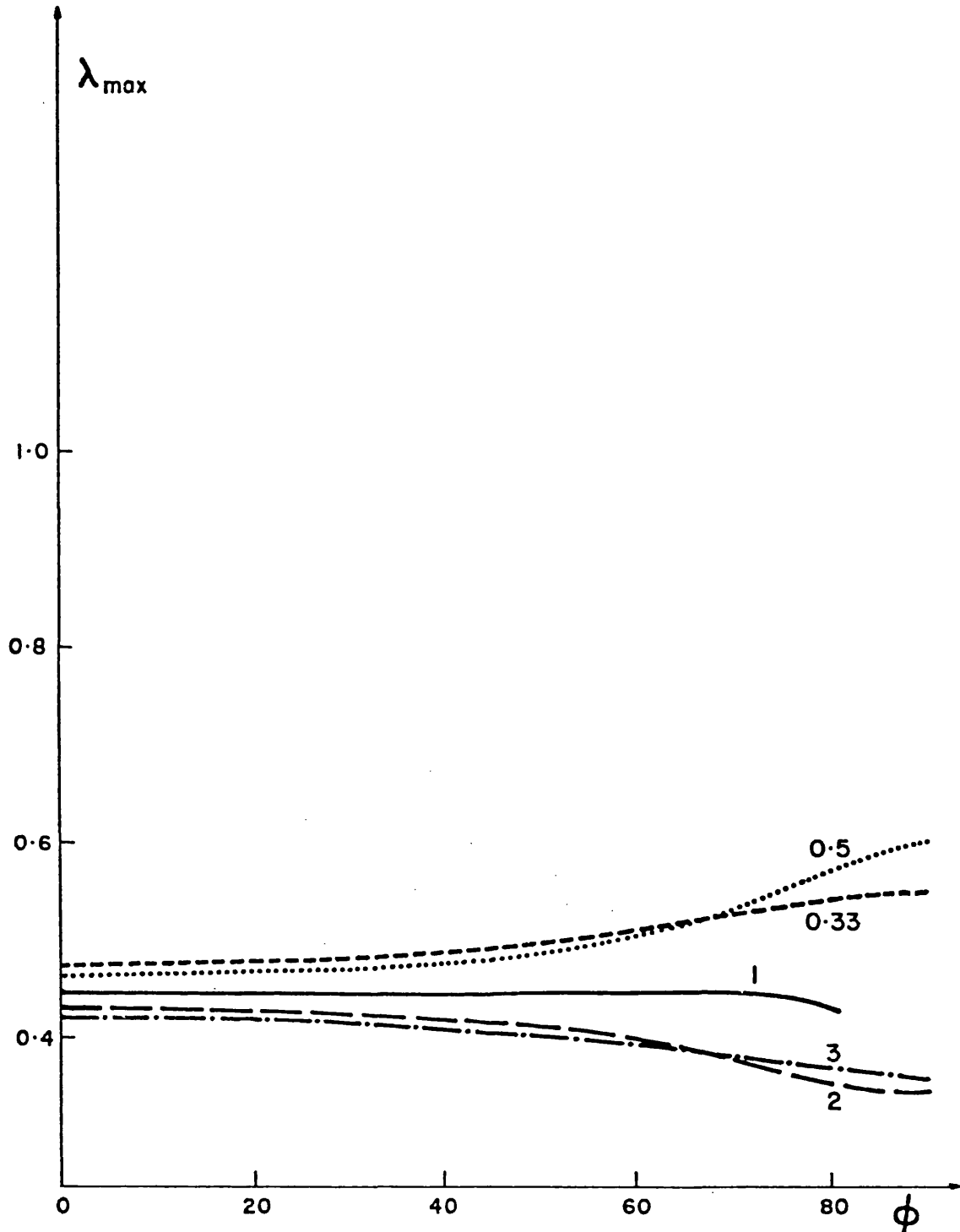


Fig. 5.8 Plots of λ_{max} values against the relative orientation (ϕ) of the two clouds for $R_\lambda = 0.8$ and for $R_p = 1, 0.5, 0.33, 2, 3$, as marked on the curves.

It was found that $(\theta_I - \theta_B)$ gives the larger values for the rotation for R_p values 2 and 3, while for the other values of R_p , i.e. 1, 0.5, 0.33, $(\theta_R - \theta_U)$ gives the larger values for the rotation of the position angle with wavelength. The position angle differences for the filter pairs therefore depend on the original characteristic parameters of the two clouds. We cannot choose filters in advance to provide the most sensitive means of detecting $\theta(\lambda)$ variations as the situation will vary from one part of the sky to another. As a result we have taken one pair represented by $(\theta_I - \theta_B)$ and investigated it with respect to ϕ for the different values of R_λ and R_p to see generally the behaviour of $\theta(\lambda)$.

Figures 5.9, 5.10, 5.11, 5.12 represent the plots of $(\theta_I - \theta_B)$ against ϕ for R_λ values 0.5, 0.57, 0.67 and 0.8 respectively.

We can see from the figures that the largest difference in the position angle is for $R_p = 1$ and this increases with ϕ for the different values of R_λ . The similarities in the behaviour of the curves for the other ratios of R_p are obvious. They increase with ϕ for the range $0 \rightarrow 70^\circ$ and then start to decrease. The smaller values of $(\theta_I - \theta_B)$ are for $R_p = 0.33$ and, generally for the lower values of ϕ , $(\theta_I - \theta_B)$ always lies within the range $0 \rightarrow 10^\circ$, for the different values of R_p and R_λ .

We have seen generally the effect of two clouds on the values of both characteristic parameters of the interstellar polarization law, i.e. K and λ_{\max} . From the figures relating K with the relative cloud orientation, ϕ , the values of K are affected in such a way that over the greater part of the range of ϕ the K values are always below 1.15 for the different cloud characteristics. This then provides a general explanation for the results obtained directly from the real data for the stars showing $\theta(\lambda)$. As we have seen, the lines representing the

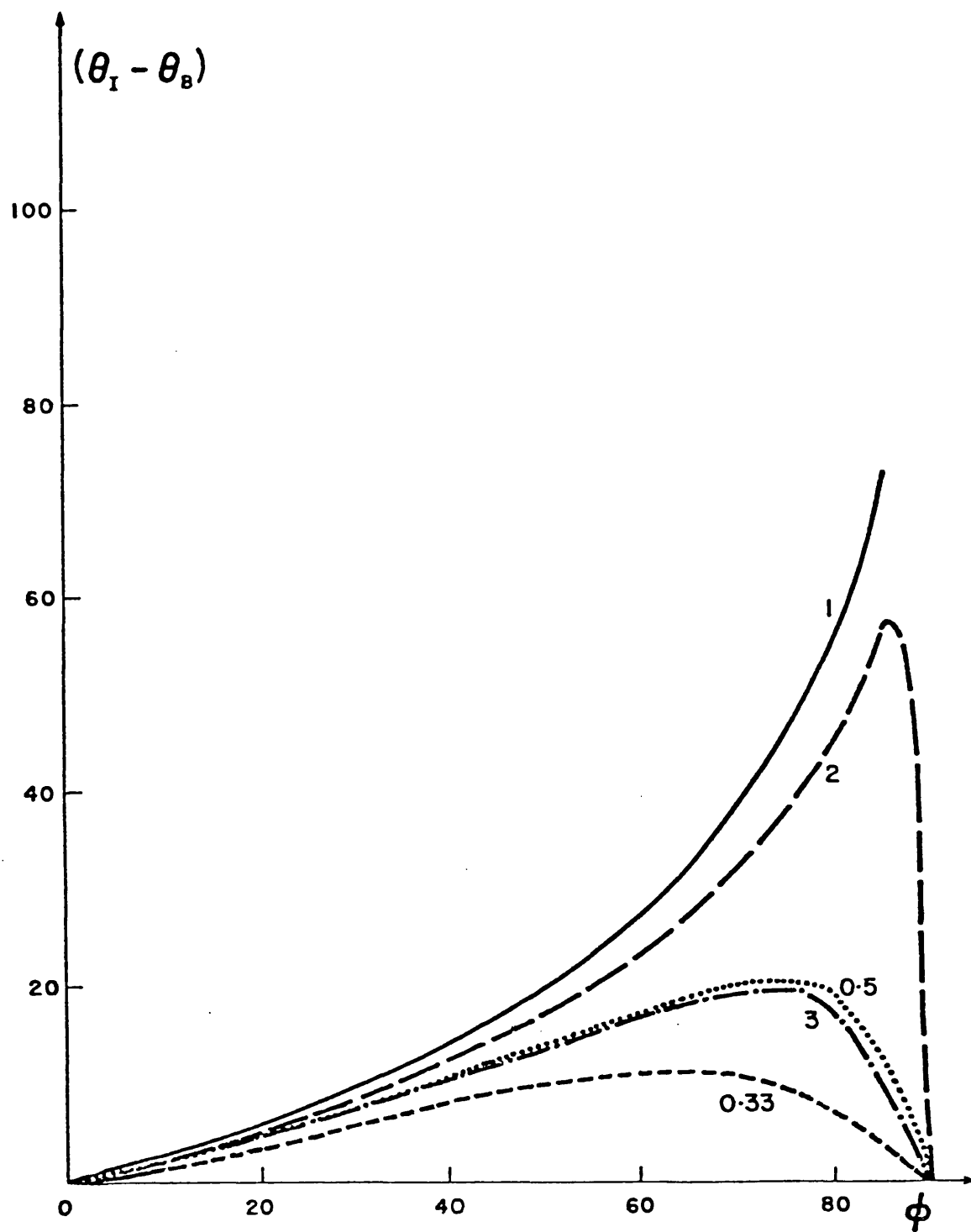


Fig. 5.9 Plots of the difference in position angles ($\theta_I - \theta_B$), of the resultant polarization against the relative orientation (ϕ) for $R_\lambda = 0.5$ and for $R_p = 1, 0.5, 0.33, 2, 3$, as marked on the curves.

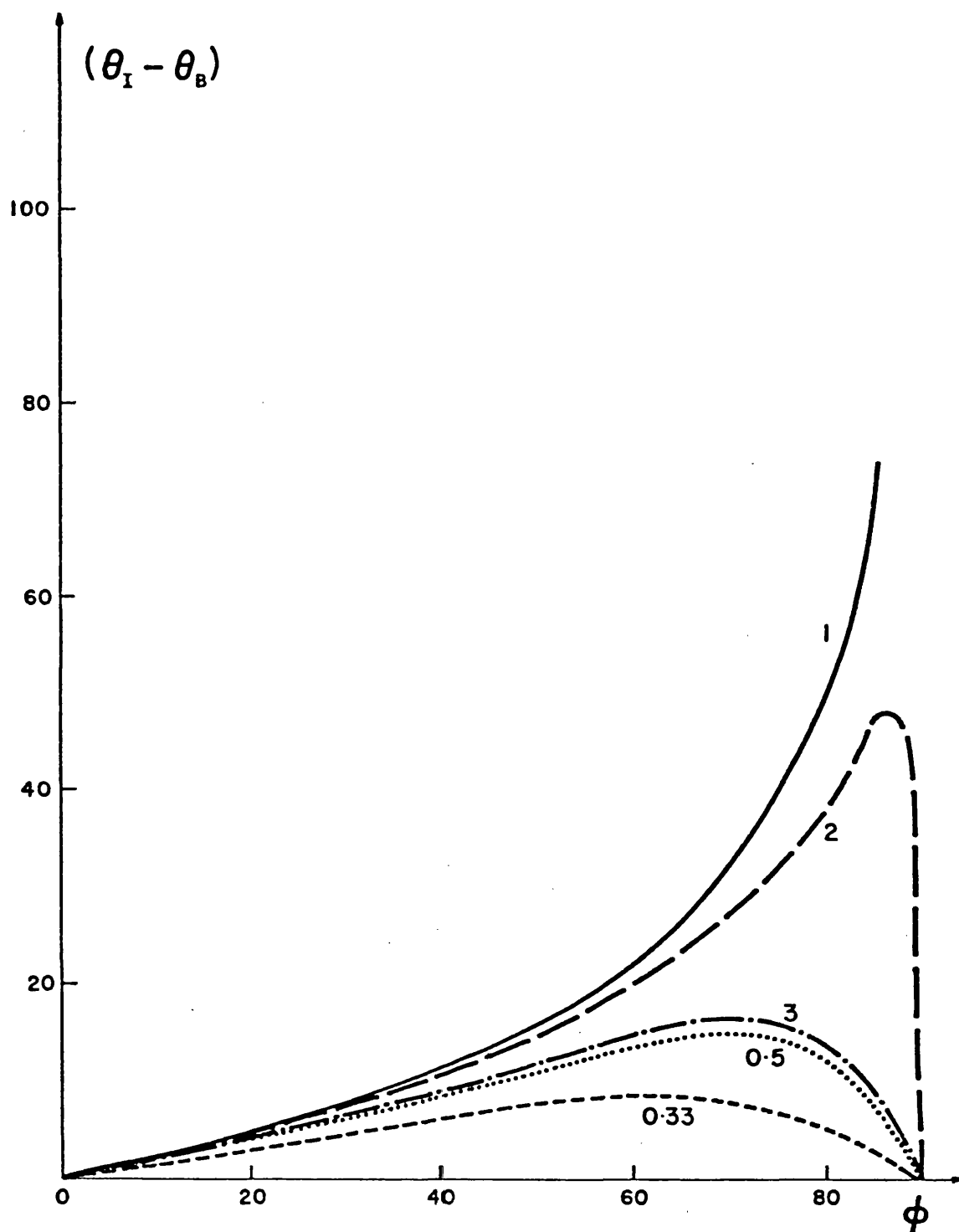


Fig. 5.10 Plots of the difference in position angles ($\theta_I - \theta_B$), of the resultant polarization against the relative orientation (ϕ) for $R_\lambda = 0.57$ and for $R_p = 1, 0.5, 0.33, 2, 3$, as marked on the curves.

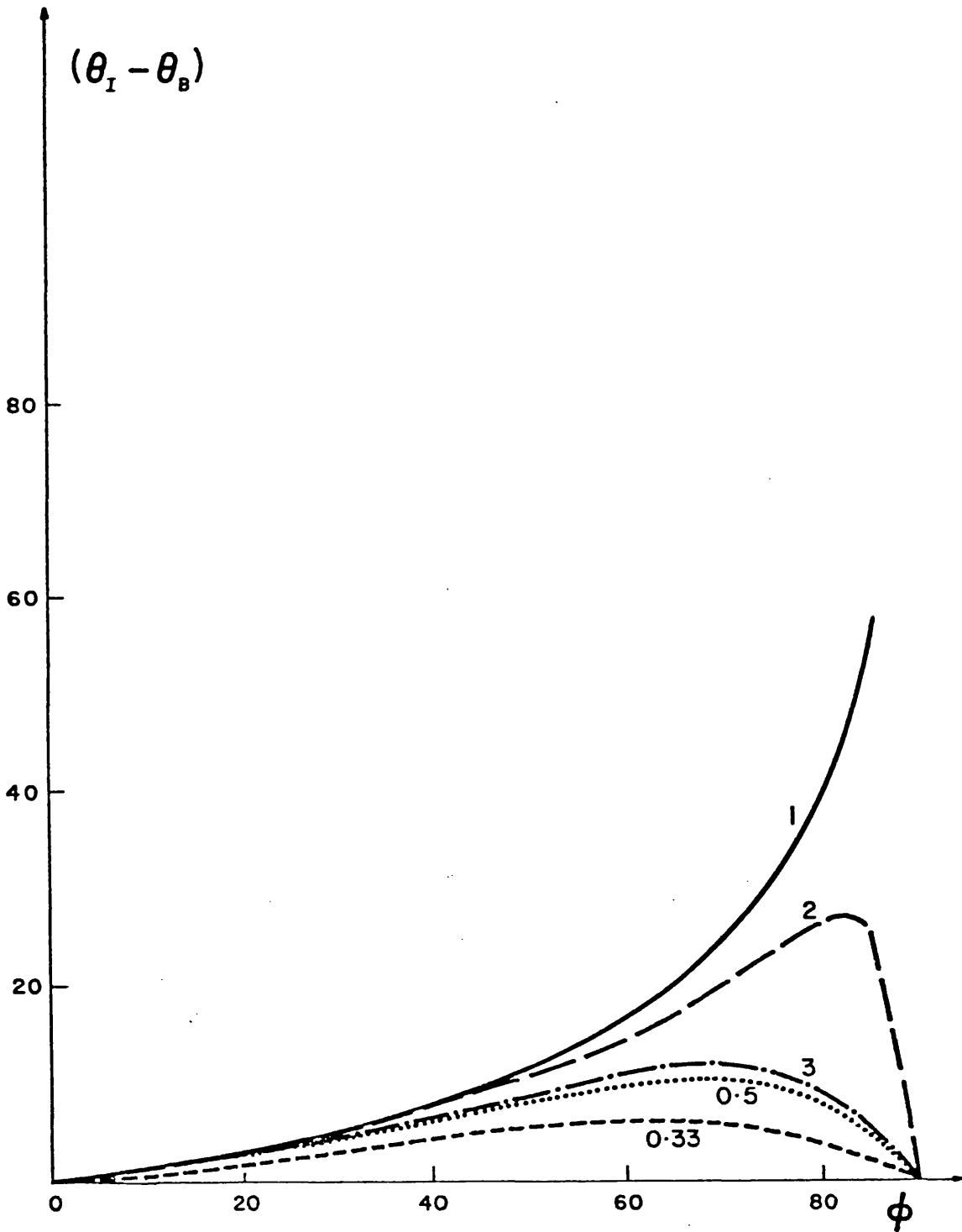


Fig. 5.11 Plots of the difference in position angles ($\theta_I - \theta_B$), of the resultant polarization against the relative orientation (ϕ) for $R_\lambda = 0.67$ and for $R_p = 1, 0.5, 0.33, 2, 3$, as marked on the curves.

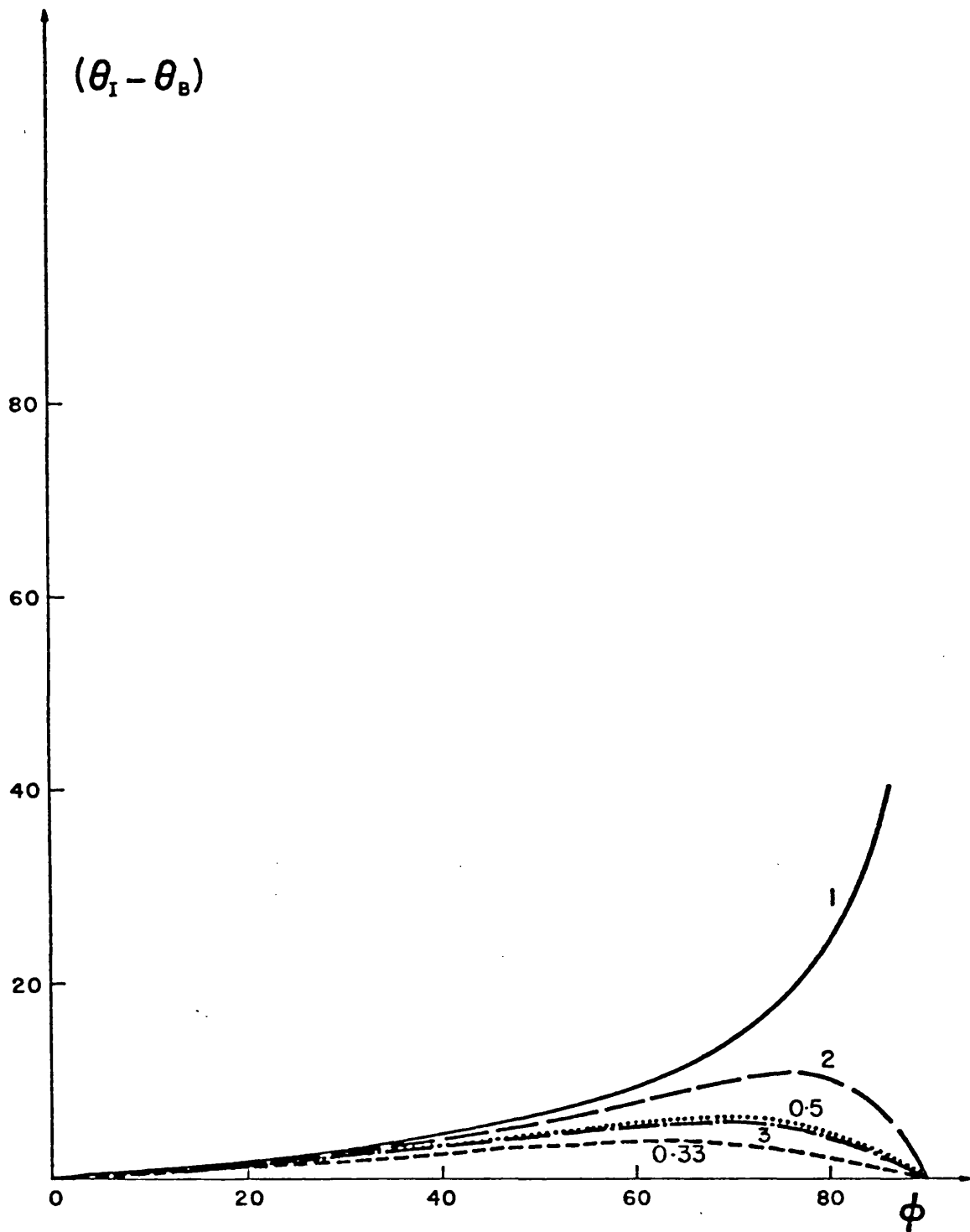


Fig. 5.12 Plots of the difference in position angles ($\theta_I - \theta_B$), of the resultant polarization against the relative orientation (ϕ) for $R_\lambda = 0.8$ and for $R_p = 1, 0.5, 0.33, 2, 3$, as marked on the curves.

relationship between K and λ_{\max} for the above data are always below the lines for normal stars.

With the current measurement precision of the $p(\lambda)$ curve it would be impossible to use a low value of K for an individual star as being indicative of the presence of complex structure in the interstellar cloud giving rise to the polarization. However, we have shown that for such stars taken as a group, overall low values ensue for K in complex cloud situations.

GENERAL SUMMARY

The investigatory research reported in this thesis has been concerned with the wavelength dependence of interstellar linear polarization and the form of its normalised behaviour, now referred to as Serkowski's Law $[p(\lambda)/p_{\max} = \exp(-K \ln^2(\lambda_{\max}/\lambda))]$.

Two aspects have been explored in the work, each based on an analysis of catalogued measurements and then complemented by theoretical studies. Firstly, Chapter 2 investigated correlations between K and λ_{\max} with Chapter 3 exploring their likely cause, and secondly in Chapter 4 effects on the parameter K when stars are observed through complex interstellar clouds were investigated and comparisons made with a simple Two-Cloud model as outlined in Chapter 5. Summaries and conclusions have been made in each of these chapters but a more general and unified summary is given here.

When spectropolarimetry is performed with a limited number of passbands and the measurements then normalised to Serkowski's Law, correlations appear relating the sharpness (K) of the $p(\lambda)$ curve with the position of λ_{\max} . These correlations appear to have gone unnoticed by the original observers who collected the data, and are reported here for the first time. Their form depends on the number of passbands used and on their effective wavelengths.

A likely cause for their existence and their variation according to the filter set used for the spectropolarimetry is the normal experimental noise associated with the measurements. The number of $p(\lambda)$ measurements for each star is small and it has been shown that if noise is present this can affect the deduced values of K and λ_{\max} in a correlated way.

For a set of stars with identical true λ_{\max} , correlations between K and λ_{\max} will ensue when the data are noisy. For a set of stars with a range of λ_{\max} , the overall correlation between the deduced values of K and λ_{\max} depends on the filter set, on the distribution of the λ_{\max} values and on the distribution of the p_{\max} values in association with the magnitude of the noise on a typical single measurement of a point on the $p(\lambda)$ curve.

This study has assumed that a normalisation of $p(\lambda)$ curves as performed by Serkowski is perfectly legitimate. This, of course, may not be the case, particularly if there is structure in the $p(\lambda)$ curve as some workers have suggested. Further study is perhaps required here. However, even if normalisation is not strictly valid, it would not affect the general conclusions arrived at here.

The presence of complicated interstellar cloud structures is thought to have been revealed by previous observers from the presence of a wavelength dependence of the position angle $\theta(\lambda)$ of the polarization. By reassessing these stars which show the effect (excluding those which might display the phenomenon as a result of an intrinsic polarization) it has been shown that the derived values of K are generally smaller than for the more usual interstellar polarization as observed for the majority of stars. A study of the Two-Cloud model shows why this is so. This exercise has been performed in a more meaningful way than by the workers who originally promoted the idea that there may be connections between $\theta(\lambda)$ and K but did not take noise sufficiently into account.

Further study of the behaviour of the interstellar polarization law must be undertaken so that more meaningful astrophysical statements might be made. At present it would seem that possible correlations between K and λ_{\max} which are interpretable on an astrophysical

basis are veiled by noise and a significant increase of measurement accuracy is called for before any major advance can be made. Improvements could be achieved by increasing the polarimetric accuracy for colour systems that have already been used or by providing a larger number of passbands. In terms of telescope application, this latter suggestion could be realised only by the use of multi-channel detectors, such as the CCD. Whether or not the necessary polarimetric precision can be achieved by these emerging devices is something which will hopefully be resolved shortly.

APPENDIX 1

The values of K and λ_{\max} for the 107 stars measured in four colours
from SMF as calculated according to the scheme in Chapter 2

HD	K	λ_{\max}	HD	K	λ_{\max}
24398	0.81	0.527	102997	1.31	0.568
30836	0.96	0.565	105071	1.25	0.584
30870	0.75	0.576	109867	1.02	0.583
32990	1.20	0.568	111193	1.51	0.553
36371	1.11	0.576	111613	0.86	0.594
37350	0.67	0.564	112244	1.35	0.667
37903	0.83	0.864	114886	1.32	0.566
38771	1.47	0.495	118522	1.06	0.576
42087	0.89	0.574	118978	1.51	0.554
42400	1.41	0.509	120908	1.11	0.625
43384	1.05	0.553	122879	1.00	0.612
46769	0.97	0.526	123335	0.95	0.609
47240	1.00	0.520	124195	1.38	0.589
51309	1.41	0.506	124314	0.85	0.583
57623	1.42	0.484	124771	0.71	0.652
58439	0.63	0.578	125788	1.33	0.540
60325	0.63	0.587	129557	1.14	0.603
61827	0.54	0.853	131918	0.90	0.530
65228	1.09	0.509	135240	1.12	0.572
69882	1.66	0.528	135591	1.39	0.574
73882	1.26	0.740	135737	1.55	0.564
74272	1.66	0.594	137709	1.04	0.530
74575	1.31	0.524	139137	0.71	0.595
74956	1.26	0.268	139160	0.86	0.577
78785	0.80	0.654	140873	0.70	0.683
79186	0.98	0.517	141637	1.26	0.569
80057	0.73	0.624	142919	1.55	0.547
81471	1.35	0.593	144217	1.22	0.626
83183	1.04	0.575	144470	1.41	0.580
84810	1.03	0.575	145206	1.31	0.568
85656	1.09	0.603	145502	1.60	0.640
85871	0.80	0.544	146323	1.06	0.595
90706	1.03	0.580	147084	0.79	0.784
90772	0.69	0.534	147889	1.53	0.715
91969	1.08	0.522	147932	1.33	0.716
92964	1.29	0.579	147933	1.31	0.668
96918	1.07	0.527	147977	1.07	0.565
98695	1.32	0.594	148379	1.05	0.616
99953	1.14	0.539	149757	1.18	0.587
102839	0.23	0.630	150168	1.16	0.551

Appendix 1 continued

HD	K	λ_{\max}	HD	K	λ_{\max}
150416	1.19	0.615	168021	1.41	0.569
150421	1.07	0.570	169420	1.24	0.667
150898	0.95	0.600	170740	0.92	0.574
154204	0.98	0.591	170764	0.87	0.545
157244	1.42	0.563	183143	1.05	0.564
157599	0.78	0.611	183344	0.97	0.550
157999	1.38	0.557	187929	1.17	0.553
159176	1.67	0.513	188001	1.14	0.580
161592	0.79	0.642	190299	0.44	0.665
161840	1.30	0.561	193150	1.42	0.568
161912	1.18	0.552	194953	0.99	0.664
162714	0.45	0.521	203532	1.05	0.567
163472	1.12	0.617	207089	1.51	0.501
			211924	1.03	0.504

APPENDIX 2

The values of K and λ_{\max} for the 73 stars measured in seven colours
and the corresponding values for the reduced data to four colours from
CGS as calculated according to the scheme in Chapter 2

HD	7-colour		4-colour	
	K	λ_{\max}	K	λ_{\max}
4180	0.47	0.471	-	-
4768	0.79	0.477	0.60	0.521
6675	-	-	0.22	0.928
7252	1.03	0.505	0.27	0.649
7902	1.28	0.495	0.90	0.514
7927	0.95	0.496	1.15	0.513
8965	1.09	0.502	0.67	0.553
9481	0.90	0.468	1.15	0.475
10898	1.12	0.485	1.53	0.491
12953	0.95	0.549	1.16	0.576
13267	1.20	0.514	0.97	0.533
13379	1.25	0.492	1.43	0.480
13470	1.13	0.503	0.50	0.449
13476	1.22	0.518	1.56	0.502
13854	1.27	0.530	0.73	0.599
14322	0.83	0.492	1.38	0.497
14433	0.91	0.489	1.01	0.506
14489	0.74	0.518	0.61	0.442
15558	1.04	0.517	0.73	0.556
16778	0.79	0.446	1.23	0.467
18326	0.73	0.518	-	-
19441	1.00	0.492	0.85	0.522
20134	0.97	0.465	0.79	0.438
20959	0.73	0.505	1.56	0.489
21291	1.07	0.519	0.93	0.514
23512	1.17	0.508	-	-
23675	1.09	0.493	1.33	0.502
24398	1.57	0.594	1.58	0.566
24432	1.27	0.574	0.91	0.571
24912	1.39	0.552	1.17	0.570
25291	0.49	0.404	0.71	0.412
25443	1.38	0.500	1.18	0.486
29866	0.91	0.608	1.02	0.568
31964	0.78	0.487	-	-
32481	1.08	0.555	-	-

Appendix 2 continued

HD	7-colour		4-colour	
	K	λ_{\max}	K	λ_{\max}
32990	1.11	0.494	1.20	0.483
33203	1.13	0.483	0.48	0.516
34078	1.17	0.532	1.31	0.566
34921	1.31	0.565	-	-
35921	1.17	0.583	1.15	0.561
36629	1.11	0.506	0.60	0.534
37202	1.56	0.626	-	-
37356	1.35	0.512	1.49	0.485
40111	-	-	0.82	0.995
41398	1.03	0.573	1.50	0.578
41637	0.66	0.509	-	-
43384	0.88	0.555	0.45	0.732
43753	0.72	0.560	0.76	0.624
47933/4	1.37	0.657	1.14	0.676
54204	0.65	0.569	-	-
54445	1.14	0.539	1.18	0.551
59176	1.40	0.499	-	-
61056	1.36	0.547	1.46	0.547
63472	0.79	0.547	-	-
83143	1.47	0.541	1.42	0.536
84915	1.28	0.520	1.37	0.556
85859	0.78	0.487	1.28	0.494
92422	1.23	0.533	-	-
97770	0.93	0.493	1.40	0.485
144217A	1.25	0.581	0.86	0.636
145502	1.43	0.677	1.56	0.661
161961	0.88	0.445	1.40	0.440
164353	1.15	0.523	0.65	0.581
192163	1.64	0.510	0.54	0.592
192641	0.21	0.307	-	-
193237	0.88	0.436	0.84	0.437
193794	0.80	0.500	1.05	0.552
198478	1.00	0.497	1.50	0.521
207260	1.23	0.522	1.11	0.469
208501	1.58	0.553	1.50	0.558
216411	1.40	0.506	1.08	0.513
218323	0.74	0.510	0.35	0.666
224014	0.95	0.549	1.16	0.576
250290	1.27	0.550	0.97	0.614
259143	1.06	0.521	1.03	0.511

REFERENCES TO FIGURES

(N.B. The numbers in brackets refer to the pages of this thesis)

- F1.1 - MATHEWSON, D. S., and FORD, V. L., 1970, Mem. R. astr. Soc. 74, 139 (7)
- F1.2 - GEHRELS, T., 1960, Astron. J. 65, 470 (9)
- F1.3 - SERKOWSKI, K., MATHEWSON, D. S., and FORD, V. L., 1975, Ap. J. 196, 261 (11)
- F1.4 - COYNE, G. V., GEHRELS, T., and SERKOWSKI, K., 1974, Astron. J. 79, 581 (13)
- F1.5 - SERKOWSKI, K., MATHEWSON, D. S., and FORD, V. L., 1975, Ap. J. 196, 261 (13)
- F1.6 - COYNE, G. V., 1974a, "Planets, Stars and Nebulae, studied with photopolarimetry", ed. T. Gehrels (Tucson: University of Arizona Press) (14)
- F1.7 - SERKOWSKI, K., MATHEWSON, D. S., and FORD, V. L., 1975, Ap. J. 196, 261 (16)
- F1.8 - SERKOWSKI, K., 1973, In "Proc. IAU Symposium No. 52: Interstellar Dust and Related Topics", ed. J. M. Greenberg and H. C. Van de Hulst (Dordrecht: Reidel) (17)
- F1.9 - CODINA-LANDABERRY, S., and MAGALHÃES, A. M., 1976, Astr. Astrophys. 49, 407 (21)
- F1.10 - - (21)
- F1.11 - WILKING, B. A., LEBOSKY, M. J., MARTIN, P. G., RIEKE, G. H., and KEMP, J. C., 1980, Ap. J. 235, 905 (23)
- F1.12 - COYNE, G. V., and McLEAN, I. S., 1975, Astron. J. 80, 702 (26)
- F4.1 - SERKOWSKI, K., MATHEWSON, D. S., and FORD, V. L., 1975, Ap. J. 196, 261 (52)

REFERENCES

(N.B. The numbers in brackets refer to the pages of this thesis)

- APPENZELLER, I, 1965, Ap. J. 141, 1390 (24)
- 1971, Astr. Astrophys. 12, 313 (19)
- BABCOCK, H. W., 1947, Ap. J. 105, 105 (5)
- BEHR, A., 1959a, Zs. für Astrophys. 47, 54 (6)
- 1959b, Nachr. Akad. Wiss. Göttingen, Math-phys. Kl.,
p. 185, Veroff. Göttingen, No. 126 (6, 22)
- BLESS, R. C. and SAVAGE, B. D., 1972, Ap. J. 171, 293 (15)
- BREGER, M., 1977, Ap. J. 215, 119 (37)
- CAPPS, R. W., COYNE, G. V., and DYCK, H. M., 1973, Ap. J. 184,
173 (24, 25)
- CARRASCO, L., STROM, S. E., and STROM, K. M., 1973, Ap. J. 182,
95 (12, 28)
- CHANDRASEKHAR, S, 1946, Ap. J. 103, 351 (5)
- CLARKE, D., and GRAINGER, J. F., 1971 "Polarized Light and Optical
Measurement", Pergamon Press (Oxford) (63)
- CODINA-LANDABERRY, S., and MAGALHÃES, A. M., 1976, Astr. Astrophys.
49, 407 (19, 28)
- COYNE, G. V., 1974a, "Planets, stars and nebulae studied with photo-
polarimetry", ed. T. Gehrels (University of
Arizona Press, Tucson) (15)
- 1974b, Astron. J. 79, 565 (24, 33, 50, 51)
- COYNE, G. V., and GEHRELS, T., 1966, Astron. J. 71, 335
(8, 33, 50)
- 1967, Astron. J. 72, 887 (8, 24, 33)
- COYNE, G. V., and KRUSZEWSKI, A., 1969, Astron. J. 74, 528 (24)
- COYNE, G. V., and WICKRAMASINGHE, N. C., 1969, Astron. J. 74,
1179 (10, 33, 50)
- COYNE, G. V., GEHRELS, T., and SERKOWSKI, K., 1974, Astron. J. 79
581 (12)

- COYNE, G. V., and McLEAN, I. S., 1975, *Astron. J.* 80, 702
(24, 25)
- COYNE, G. V., TAPIA, S., and VRBA, J. F., 1979, *Astron. J.* 84,
356 (19)
- DAVIS, L., and GREENSTEIN, J. L., 1951, *Ap. J.* 114, 206 (28)
- DYCK, H. M., and JONES, T. J., 1978, *Astron. J.* 83, 594 (20)
- FISHER, R. A., and YATES, F., 1963, "Statistical Tables for Bio-
logical, Agricultural and Medical Research",
Oliver & Boyd (Edinburgh) (33)
- GEHRELS, T., 1960, *Astron. J.* 65, 470 (8, 29)
- GEHRELS, T., and SILVESTER, A. B., 1965, *Astron. J.* 70, 579
(8, 50)
- GREENBERG, J. M., 1968, "Nebulae and Interstellar Matter", edited
by B. M. Middlehurst and L. H. Aller (U. Chicago
Press) p. 221 (12)
- 1978, "Cosmic Dust", Ed. J. A. M. McDonnell,
Wiley Pub. 1978, Chapter 4, p. 187 (18)
- HALL, J. S., 1949, *Science* 109, 166 (4, 5)
- HALL, J. S., and SERKOWSKI, K., 1963, "Basic Astronomical Data,
Stars and Stellar Systems" Vol. III (Univer-
sity of Chicago Press) p. 293 (6)
- HILTNER, W. A., 1949a, *Science* 109, 165 (4, 5)
- 1951a, *Ap. J.* 114, 241 (5)
- 1954a, *Ap. J.* 120, 41 (5)
- 1954d, *Ap. J.* 120, 178 (5)
- 1956, *Ap. J.*, Suppl. 2, 389, No. 24 (5)
- KRUSZEWSKI, A., 1963, *Acta Astron.* 13, 100 (19)
- MARKANNEN, T., 1977, *Obs. Astrophys. Lab., Univ. Helsinki, Rep. 1/*
1977 (19)
- MARTIN, P. G., 1972, *Mon. Not. R. astr. Soc.* 159, 179 (18)
- 1974, *Ap. J.* 187, 461 (28, 50, 53, 55, 63)

- MARTIN, P. G., 1978, "Cosmic Dust, its Impact on Astronomy",
Clarendon Press (Oxford) (53, 63)
- MARTIN, P. G., and ANGEL, J. R. P., 1976, Ap. J. 207, 125 (55)
- MARTIN, P. G., ILLING, R., and ANGEL, J. R. P., 1972, Mon. Not. R.
astr. Soc. 159, 191 (18, 50)
- MATHEWSON, D. S., and FORD, V. L., 1970, Mem. R. astr. Soc. 74,
139 (6, 51)
- McLEAN, I. S., and CLARKE, D., 1979, Mon. Not. R. astr. Soc. 186,
245 (25)
- McMILLAN, R. S., and TAPIA, S., 1977, Ap. J. 212, 714 (19, 55)
- MORGAN, W. W., WHITFORD, A. E., and CODE, A. D., 1953, Ap. J. 118,
318 (6)
- POECKERT, R., 1975, AP. J. 196, 777 (24)
- SCHEFFLER, H., 1967, Z. Astrophys. 65, 60 (12)
- SERKOWSKI, K., 1962, "Advances in Astronomy and Astrophysics"
Vol. 1 (Academic Press N.Y.) p. 289 (8, 50)
- 1965, Ap. J. 142, 793 (24)
- 1968, Ap. J. 154, 115 (15, 50)
- 1973, In "Proc. IAU Symposium No. 52: Inter-
stellar Dust and Related Topics", ed. J. M.
Greenberg and H. C. Van de Hulst (Dordrecht:
Reidel) (12, 15)
- SERKOWSKI, K., GEHRELS, T., and WISNIEWSKI, W., 1969, Astron. J.
74, 85 (33)
- SERKOWSKI, K., MATHEWSON, D. S., and FORD, V. L., 1975, Ap. J. 196,
261 (10)
- SERKOWSKI, K., and ROBERTSON, J. W., 1969, Ap. J. 158, 441
(8, 10)
- SHAH, G. A., 1967, Ph.D. thesis, Rensselaer Polytechnic Institute,
Troy, New York. (12)
- SHAKHOVSKOJ, N. M., 1962a, Astron. Zhurn. 39, 755 (Transt.
Soviet Astron. 6, 587) (24)

- SHAKHOVSKOJ, N. M., 1964, Astron. Zhurn. 41, 1042 (Transt.
Soviet Astron. 8, 833) (24)
- TREANOR, P. J., 1963, Astron. J. 68, 185 (8, 50)
- VERSCHUUR, G. L., 1974, "Planets, stars and nebulae studied with
photopolarimetry", ed. T. Gehrels (Univer-
sity of Arizona Press, Tucson) p. 960 (6)
- WILKING, B. A., LEBOSKY, M. J., MARTIN, P. G., RIEKE, G. H., and
KEMP, J. C., 1980, Ap. J. 235, 905 (20)
- YOUNG, H. D., 1962, "Statistical Treatment of Experimental Data",
McGraw-Hill Book Comp. Inc. (New York) (33)

LIBRARY
UNIVERSITY OF ARIZONA
TUCSON, ARIZONA